

Energy & Environmental Science

Accepted Manuscript

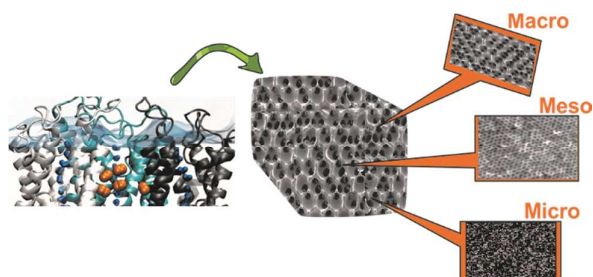


This is an *Accepted Manuscript*, which has been through the Royal Society of Chemistry peer review process and has been accepted for publication.

Accepted Manuscripts are published online shortly after acceptance, before technical editing, formatting and proof reading. Using this free service, authors can make their results available to the community, in citable form, before we publish the edited article. We will replace this *Accepted Manuscript* with the edited and formatted *Advance Article* as soon as it is available.

You can find more information about *Accepted Manuscripts* in the [Information for Authors](#).

Please note that technical editing may introduce minor changes to the text and/or graphics, which may alter content. The journal's standard [Terms & Conditions](#) and the [Ethical guidelines](#) still apply. In no event shall the Royal Society of Chemistry be held responsible for any errors or omissions in this *Accepted Manuscript* or any consequences arising from the use of any information it contains.

Table of Content Entry:

Polymers and biopolymers via non-templating synthesis emerging as new strategy to access hierarchically porous carbons for a range of energy applications

Hierarchically Porous Carbon Derived from Polymers and Biomass: Effect of Interconnected Pores on Energy Applications

Saikat Dutta,^{a*} Asim Bhaumik,^{b*} Kevin C.-W. Wu^{a*}

^aDepartment of Chemical Engineering, National Taiwan University, Taipei, Taiwan 10617

E-mail: saikatdutta2008@gmail.com, kevinwu@ntu.edu.tw Tel.: +886-33669534

^bDepartment of Materials Science, Indian Association for the Cultivation of Science, Jadavpur, Kolkata-700032

E-mail: msab@iacs.res.in, Fax: (+91) 33-24732805

1. Introduction

Naturally occurring species are employed as resource for a wide range of materials which suggests a significant fraction of complex functionalities of living systems bank on their hierarchical structures.¹ Compared to conventional porous materials with uniform pore dimensions that can be adjusted over a wide range of length scales, hierarchical porous materials with well-defined pore dimensions and topologies offer minimized diffusive resistance to mass transport by macropores and high surface area for active site dispersion over the micro- and/or mesopores.² Such a novel type of interconnected porous carbon materials with 1D to 3D network are currently attracting a great conduct of interest due to their potential technological application profile ranging from electrochemical capacitors,³ lithium ion batteries,⁴ solar cells,⁵ hydrogen storage systems,⁶ photonic material,⁷ fuel cells,⁸ and sorbents for toxic gas separation.⁹ Good electrical conductivity, high surface area, and excellent chemical stability are certain unique physicochemical properties which are responsible for micro/nanostructured porous carbon to be highly trusted candidate for emerging nanotechnologies. Novel porous carbon materials with controlled morphology, porosities, and architectures, especially carbon frameworks with hierarchical porosity, namely, mesopores in combination with macropores or micropores is highly desired due to their unique structural features compared with carbon materials containing macropores connected with mesopores. The design of hierarchical nanostructured carbons (HNCs) with tailored macropores/mesopores and electron donating element doping was emerged

as a promising field of further investigation delivered with extensive scope. The most commonly used synthetic technique for fabrication of HNCs is “nanocasting” (hard templating) with hierarchical nanostructured silica (HNS) as template to impregnate with an appropriate carbon source, followed by carbonization of the composite, and subsequent removal of the template. Primarily, apart from accessing ordered mesoporous carbons (OMCs) (Figure 1(a)), the same with macro/mesoporous arrays, disordered HNCs with macro/mesoporosity, and hollow macroporous core/mesoporous shell were also obtained using nanocasting strategy.¹⁰

Major challenges for fabrication of ordered HNCs with 3D-interconnected macroporous and mesoporous structures consist in complexity of interconnected meso/macroporous HNSs with long-range order. Particularly interesting are those nanostructured porous carbon materials¹¹ or carbon materials exhibiting three-dimensional (3D) hierarchical porous textures (containing pores at different scales, from micropores to mesopores, up to macropores) that combine high specific surface areas with proper channels and allow efficient diffusion of any substance (e.g., analytes, adsorbates, electrolytes etc) to the entire surface of the material.¹² Meso- and macro porosity exert significant effect in introduction of more graphitic, nitrogen doped carbon into the mesopores of a three-dimensionally ordered macroporous monolithic carbon (3DOM/m C) by chemical vapor deposition to produce a monolithic carbon/carbon nanocomposites material (3DOM/ m C/C) ((Figure 1(b)).^{12(a)} Constructing different nanoscaled pores with interconnections are very important and that majorly depends on the synthetic strategies of hierarchically porous carbons (HPCs) and level of the microstructure. To date, well-defined HPCs are accessible via hard-/soft-templating approaches and post-activation combined methods. For example, Cheng and co-workers prepared a 3D periodic hierarchical porous graphitic carbon by using alkaline system consists with $\text{Ni}(\text{OH})_2/\text{NiO}$ -phenolic resin as a hard template (Figure 1(c)),¹³ and Lu and co-workers described the HPCs obtained by post-activation of Pluronic F127-templated phenolic resin.¹⁴

However, most of the templates are expensive and the post-synthetic removal of the template to produce a carbon replica requires additional processing steps that are usually severely time-consuming and harmful for environmental safety. These limitations impart to HPCs an uncompetitive price-to-performance ratio as compared with other materials and thus limit their commercial viability. Obviously, the problem can be fully eliminated with the incorporation of hierarchical porosity by using any auxiliary template. Therefore, building

controllable hierarchical porous structure from biorenewable source through a template-free method is a great current challenge.

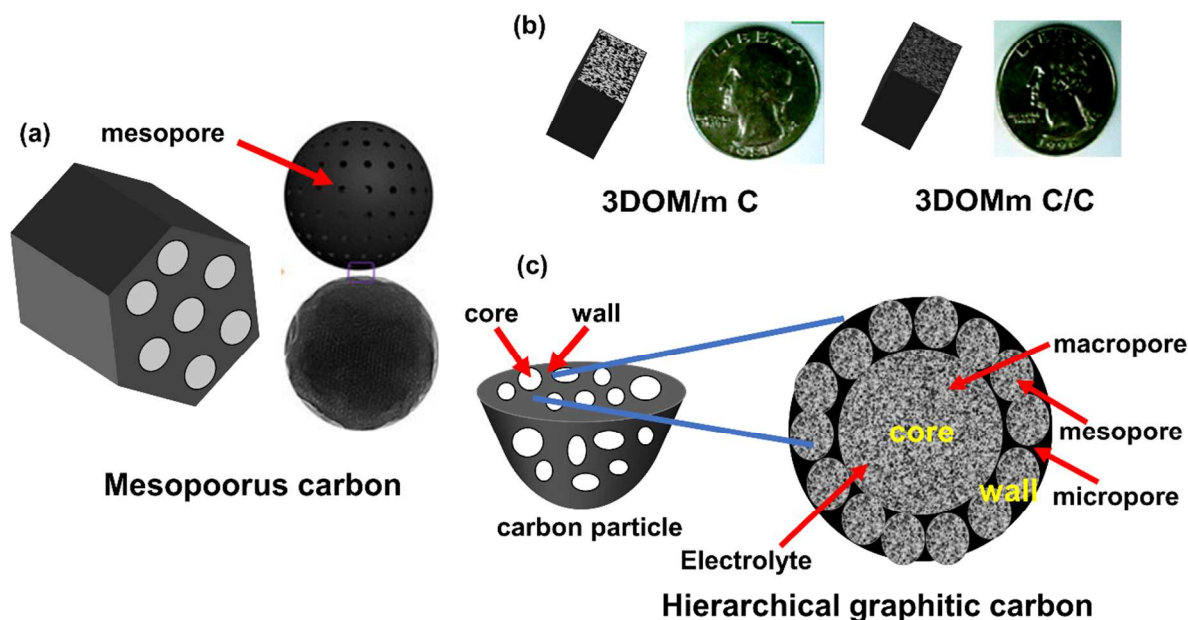


Figure 1. Schematic representation of (a) 2D mesoporous carbon, (b) three-dimensionally ordered macroporous monolithic carbon (3DOM/m C) and a monolithic carbon/carbon nanocomposites material (3DOM/ m C/C), (c) 3D hierarchical porous texture of core, walls, and pores (mesoporous walls, microporous, and macroporous cores) of hierarchically porous graphitic carbon materials.

2. Scope

In this review, soft-templating, hard-templating as well as non-templating strategies developed for the fabrication of hierarchical porous carbon nanomaterials from various carbon-rich precursors such as polymers, copolymers and biomass-derived polymers as carbon source are surveyed. The aim of this article is to emphasize the newly explored carbon precursors and naturally occurring biopolymers for their wondrous future prospects in deriving nanostructured HPC materials. Subsequently, a perspective on advanced applications of HPCs for emerging areas of energy storage and generation including reversible CO₂ capture for clean energy technology, carbon photonic crystals, lithium-sulfur batteries, and supercapacitors is organized. The review will mainly focus on the application profiles of the hierarchical porous carbons

emphasizing on the effect of the interconnectivity of the pore-network on the efficiency of the materials for a specific application. Thus this would help in better understanding of the interconnected pores-property inter relationship. A comparative description of synthesis strategies of HPCs and ordered mesoporous carbons (OMCs) is provided which would emphasize the factors responsible for the growth of hierarchical porous nanostructures unlike the nanostructure of OMCs. The article is completed with brief discussion on the applications of HPCs derived from biorenewable sources and conclusion.

3. Fabrication of HPCs from Polymers and Biomass

3.1. Hard-Templating

A large number of techniques were explored for the access of HPCs with combined macro- and mesoporosity majorly based on the dual templating strategy where two templates with dimensions at different length scale are combined to originate multimodal pores.^{14,15} Primarily, these strategies involve nanocasting (hard templating) or a combination of hard and soft templates.^{16,17} Among other techniques, template replication of hierarchical inorganic materials^{12(a)} and sol-gel^{18,19} methods are known. A major challenge to date has been the development of HPCs with very high surface areas, pore volumes and porosities at all three different length scales: macro-, meso-, and micro in a simple material platform. Additional challenges with the synthesis techniques include the requirement to synthesize porous inorganic materials or special nanoparticles as hard templates which involve time consuming multiple steps and high expenses. Furthermore, most of the already explored soft-templates are based on rather expensive and non-renewable surfactants and block-copolymers. Moreover, the size of the mesopores may be difficult to tune due to aggregation of the nanoparticles carbon precursor matrix. Ice templating has been known for its potential for fabricating macroporous and hierarchical nanostructures.^{20,21} Based on the dual templating strategy, combined ice templating beside a hard template (colloidal silica) followed by physical activation generates excellent interconnected macro-, meso- and microporosity, respectively as shown by Estevez and co-workers.²² It is witnessed that combined silica particles (hard template) and glucose molecule (as carbon source) were expelled away from growing ice crystals (hard template) by plunging the mixture into liquid nitrogen. Glucose-silica composite scaffold offers inter-connected macroporous carbon-silica structure which remain intact during pyrolysis and silica etching

(Figure 2a). Most importantly resulting HPC scaffold contains macroporous walls made of interconnected mesoporous carbons (Figure 2b). A distinct advantage is that this approach minimizes the aggregation of hydrophilic silica particles by instantaneous locking within the glucose matrix and subsequent carbonization. The process offers bimodal nature of mesoporosity witnessed in the pore size distribution when using silica particle of different size. Moreover, pore size of the carbon material increases due to the aggregation during freezing. Ice-template-silica particle derived HPCs contain macro- and mesopores (multimodal) dominated texture with tight control and tenability of porosity in terms of size and extent. This offers HPC monolith with desired shapes and size along with high pore volumes and large pore sizes making this as excellent candidates for amine based CO₂ capture.

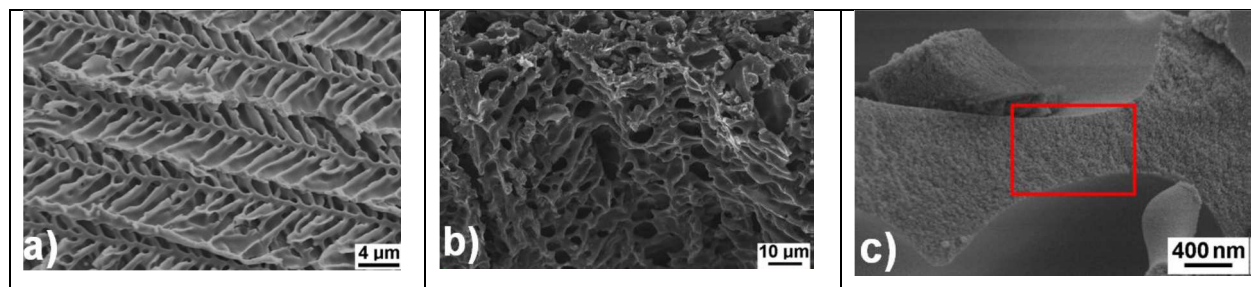
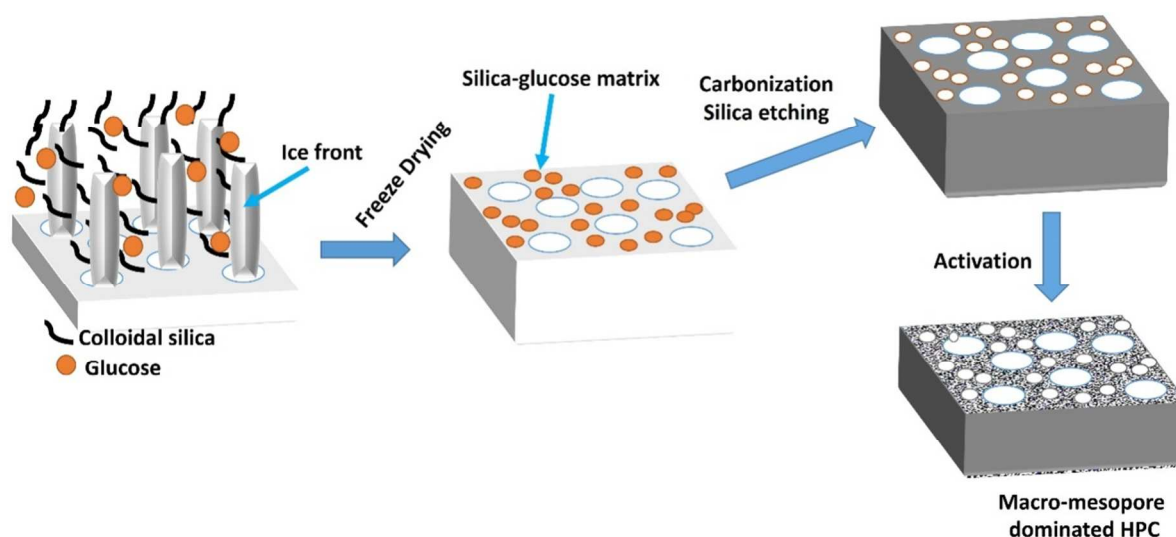


Figure 2. Ice-templating route to access HPC dominated by macro and mesopores. SEM images a) glucose-silicacomposite, b) carbonized HPC materials (HRSEM), c) macroporous walls of the

glucose-silica material. (Figure 2a, 2b, 2c are reproduced from SI of reference 25 with permission, Copyright, RSC 2013)

3.2. Soft-Templating

Soft-templating can be a good alternative method to access HPCs in which pore structure collapse can be minimized using molecular species in the reaction media, which after gelation, stabilizes the pores from collapsing during drying the carbonization.²³ It is proposed that that micelles formed during the process and act as template for constructing the pores. HPCs of tunable pore size through soft-templating can be obtained when utilized a cationic polyelectrolyte poly(diallyldimethylammonium) chloride (PDADMAC) as soft template while using resorcinol-formaldehyde (RF) gel as carbon source.²⁴ There is an stabilizing effect of the cationic polyelectrolyte on the sol-gel nanostructure in which porosity of the gel is maintained during the drying process. Introduction of a scaffold for the mass production of HPC monolith while using triblock copolymer F127 as soft template and phenol-formaldehyde (PF) resin as carbon precursor offers HPCs decorated with micro- and meso-porosity prepared by surface coating and solvent evaporation-induced self-assembly (EISA).²⁵ In this soft-templating method of transformation of monolith into the HPC with ordered mesopores through thermopolymerization, hierarchical porous architecture is retained while the bulk structure of the scaffold (sugarcane bagasse) was destroyed. This soft-templating method simplifies greatly the production of porous carbon by making unnecessary to use complex drying procedure. Dual templating (hard-soft) approach can give rise to HPC with new nanostructure. Flow-enabled self-assembly approach using hierarchically assembled amphiphilic diblock copolymer micelles and inorganic nanoparticles which were crafted over large areas and the process results one-step hierarchical self-organization, i. e. parallel threads comprising amphiphilic diblock copolymer micelles and inorganic nanoparticle on the nanometer scale.²⁶ This type of hierarchical assembly obtained from block copolymer micelles would open up ways to fabricate novel HPCs.

To this far, only few cases of HPC fabrication using polymers and biomass-derived molecule as carbon source and hard- or soft-templating strategy was investigated. Among this, dual templating (hard-soft) found more promising for fabricating interconnected porosity. The major hurdle is the efficient fabrication of a hierarchical nanostructured silica or other template with tailored hierarchical porosity of meso/macropores. Additional difficulties associated with

hard templating process is the template removal under concentrated basic condition. Either decomposition or etching are the strategies to remove the hard template. Any porous inorganic template removal requires time consuming multiple steps. At the same time, most of the soft templates used for self-assembly are based on surfactants and block-copolymers, which rather expensive and non-renewable. In some cases, size of the mesopores can also be difficult to fine tune because of aggregation of the nanoparticles in the polymerizing carbon precursor matrix.²⁶ In addition, soft-templating techniques like sol-gel suffer from the critical drawback associated with the long synthesis time required for gelation, solvent exchange and supercritical drying. Further, major difficulties associated with the template removal in the nanocasting and soft-templating methods²⁷ irrespective of the carbon source, efficient non-templating approach of accessing porous carbons with a controllable pore structure and good mechanical strength is highly desirable. Thus, self-assembly process of carbon source without a surfactant in the reaction system is a challenging task.

3.3. Non-Templating

The 3D nanoscaled architecture not only provide a continuous electron pathway to ensure good electrical contact, but also facilitate ion transport by shortening diffusion pathways.²⁸⁻³¹ The major challenge for development of carbon based electrode materials for high-performance energy-storage, is how to achieve the desirable properties such as large surface area, high conductivity, efficient porosities in micro-, meso- or macro-pores, 3D nanoarchitecture and high-level heteroatom-doping. Among the non-template based strategies, a noteworthy approach based on the polypyrrole (PPy) microsheets as precursor for carbon and KOH activation offers HPC with hierarchical porous microstructures exhibiting macro-porous frameworks, mesoporous walls, and micro-porous textures. This pore network is prosperous for diffusion of the active ions.³²

In PPy derived HPCs, mesopores with diameter 10-50 nm was detected in carbon walls which are wider as compared to that of the traditional HPCs and activated carbons (pores smaller than 4 nm). This is due to the efficient phase separation between the hydrophobic carbon and water during the KOH activation process. This material also exhibits an annealing temperature dependent stability of the pore network. For example, pore widening maximum 500 nm at 700 °C was recorded. Among the advantages of HPCs derived from PPy sheet, major is high surface

area that leads to sufficient electrode/electrolyte interface to form electric double layers. Another advantage is the hierarchical porous network not only ensures the fast ion diffusion by shortening the diffusion pathways, also utilized macroporous frameworks as ion-buffering reservoirs, mesoporous walls as ion-highways for fast ion transmission, and microporous textures for charge accommodation. Additionally, these features also provides continuous electron pathways, important for achieving high-rate performances. Non-templating chemical activation method has also offered porous carbons with micro- (~ 1.2 nm)³³ and mesoporosity and which are obtained from the hydrothermal carbonization of polysaccharides (starch and cellulose). Bioresourced carbon can also be derived from Yeast which contains an amorphous matrix and fibrillar network that burnt off to deliver carbon material.³⁴ Here, the fraction of narrower micropore (< 0.7 nm) formation depends on the degree of activation of the carbons.

For fabrication of polystyrene-derived HPC (PS-HPC) with a unique hierarchical porous nanonetwork depends on constructing carbonyl cross-linking bridges between PS chains via template-free method.^{2,35} Fabrication of spherical HPC by linear polystyrene depends on the construction of carbonyl ($-\text{CO}-$) crosslinking bridges between linear polystyrenes in which carbonyl crosslinking bridges simultaneously provides the resulting hierarchical porous polystyrene (HPP) with a high crosslinking density and sufficient oxygen atoms. This forms hierarchical pore structure during carbonization.^{2,3,4,36} Introducing an appropriate pre-cross linking density into polystyrene nanospheres could minimize the chances of distortion of spherical shapes during the process of swelling and crosslinking. Indeed, $-\text{C}_6\text{H}_4-$ crosslinking bridges by incorporating divinylbenzene (DVB) ensures stability of styrene-divinyl benzene (St-DVB) copolymer nanospheres in spherical shape that results mesopores of dimension 2-50 nm via the compact aggregation of St-DVB nanospheres and its size.³⁶ This non-templating strategy is quite different from PPy microsheet-derived HPCs which majorly depends on the chemical activation method for the 3D hierarchical pore construction. In this process, $-\text{C}_6\text{H}_4-$ crosslinking bridges provides stability of the nanospheres during swelling and $-\text{CO}-$ crosslinking bridges offers good nanostructure inheritability in carbonization. In this process, access to the small sized monodisperse nanoparticles are essentials for fabricating HPC with mesopores after aggregation of the particles. Dispersion polymerization and delay in addition ensures the formation of smaller nanoparticles (55 nm) by using low styrene nucleation concentration which further ensures spherical shapes of St-DVB nanospheres. Carbonyl ($-\text{CO}-$) crosslinking bridges in CCl_4 results

in hierarchical pore network by intra-/inter-sphere crosslinking of polystyrene chains of nanospheres (Figure 3). As a result, the intra-sphere space will be subdivided into numerous micropores by the as-constructed intra-sphere crosslinking bridges. By the attack carbocations (CCl_3^+) on the surface of nanospheres resulting inter-sphere $-\text{CCl}_2-$ crosslinking bridges and stacking of nanospheres in certain orientation leads to 3D network nanostructure containing micropores inside the nanospheres. Formation and growth of network nanoparticles from a template-free method involves crosslinking of linear polystyrene chains that are hard to control in terms of the shape and size distribution of the particles which limits the fabrication of HPCs with tunable structures.

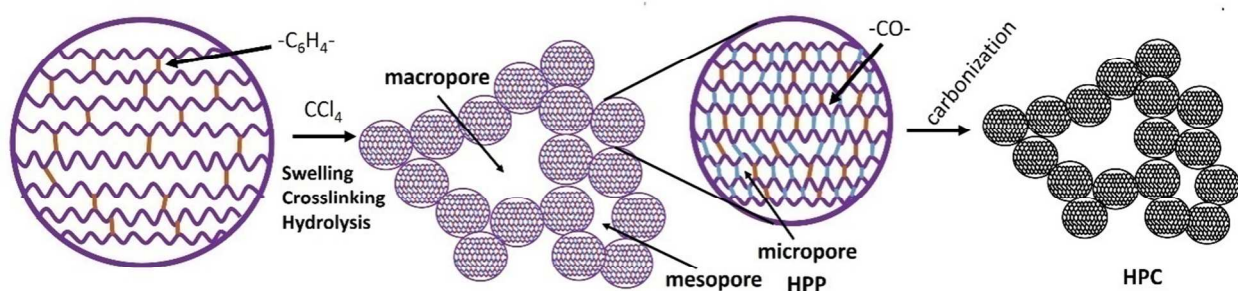


Figure 3. Mechanism for the formation of hierarchical porous carbon (HPC) by intra-/inter-sphere crosslinking of polystyrene chains of nanospheres via a template-free method.

A hierarchical porous network of 3D interconnected micro-, meso-, and macropores can also be accessible from the carbonization of hierarchical porous polyaromatic precursor obtained from aromatic hydrocarbons (AHC) (polynaphthalene, polypyrrole).³⁷ When the origin of hierarchical pore network in aggregates of carbon spheres is based on the methylene bridges between phenyl rings, a fast ion transport/diffusion behavior and increased surface area usage in electric double-layer was found. Specialty of this AHCs derived HPCs depends on its micropores in 3D interconnected network inside the cross-linked AHC microspheres imparting exceptionally high electrochemically accessible surface area for charge accumulation. Method of HPCs obtained through methylene bridges between aromatic rings offers maximum surface area $455 \text{ m}^2\text{g}^{-1}$ (S_{BET}) which is indeed less than that can be obtained via $-\text{CO}-$ bridged polystyrene copolymer derived HPCs ($S_{\text{BET}} 887 \text{ m}^2\text{g}^{-1}$). The total pore volume (max $0.41 \text{ cm}^3\text{g}^{-1}$) of AHCs derived HPC is very less than that of the polystyrene copolymer derived HPCs which indicates

the advantages of the introduction of –CO–crosslinking bridges for the nanostructure inheritability during carbonization. Superior electrical conductivity offered by AHCs derived HPC is perhaps due to the formation of aggregates of spherical carbon spheres composed of turbostratic carbon with weakly ordered graphitic microstructure which is different from origin of micropores from direct carbonization or activation process. Turbostratic carbon³⁸ is generally a variant of h-graphite, stacked up by graphene layers with regular spacing but different stacking ordering degree. This weakly order graphitic microstructure can enhance the electrical conductivity.

HPCs can be obtained via hydrothermal carbonization (HTC) of glucose and fructose as carbon source which generally undergoes dehydration to 5-hydroxymethylfurfural³⁹ under HTC condition and resulting polyfuran type aggregate into secondary spherical particle of the final size. In this non-templated process, poly(ionic liquid)s (PIL) act as a stabilizer of primary nanoparticles formed at the initial stage and allow only growth by further addition of monomers.⁴¹ This occurs by electrostatic repulsion exerted by the PIL to minimize agglomeration by lowering the particle size to < 50 nm. From this stage, final hierarchical particle (Figure 4) forms like the formation of ordered mesoporous carbons (OMCs) through the use of block copolymer as soft templates typically using resorcinol-formaldehyde resins as carbon source.⁴⁰ Multivalent binding power of PILs has been explored over ILs for the formation of pores apart from its catalytic effect on the HTC process.⁴¹ It reveals that in PILs-based HTC process, macromolecular architecture of PILs and nature of anion control the formation of HPCs with desired pores network and functionality.

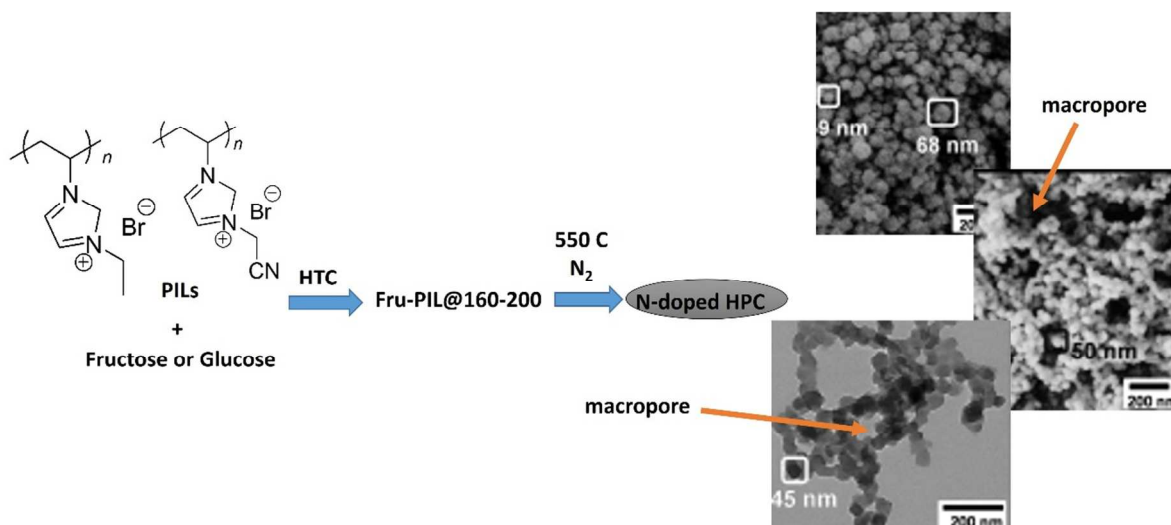


Figure 4. Hierarchical porous N-doped carbon nanostructure using PILs as multipurpose agent (Figure is reproduced from reference 41 with permission, Copyright Wiley-VCH, 2013).

In order to optimize the structural features of hierarchical porous carbon monolith (HCM), an approach of incorporating host foreign components in macropores with particularly those showing high CO₂ capture capability would be a novel strategy. Synthesis of such HCM based composite allows further improvement on its volumetric CO₂ capture ability. A recent study of incorporating metal-organic frameworks into the hierarchical pores of HCM with a MOF (Cu₃(BTC)₂(BTC = 1,3,5-benzenetricarboxylic acid), known for its promising CO₂ capture ability, was reported (Figure 5).⁴² In HCM-Cu₃(BTC)₂ composites, macropores of HCM matrix provides a microenvironment for the growth of Cu₃(BTC)₂ crystallites and dispersed within HCM matrix which involves a restriction effect by carbon skeleton of HCM. HCM's polar surface and high bulk density with incorporation of MOF crystallites in the macropores of HCM is a novel strategy for practical CO₂ adsorption.

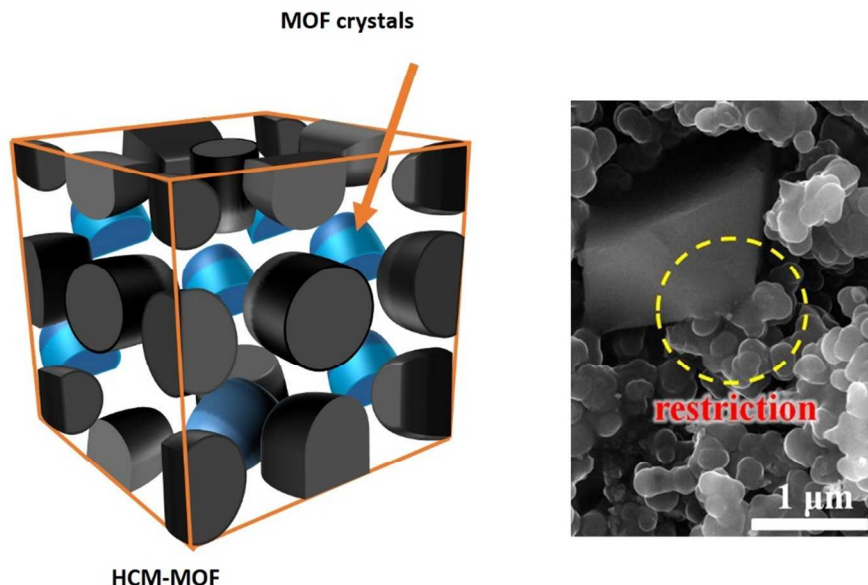


Figure 5. HPC monolith containing MOF crystallite inside the macropores and SEM micrograph HPC-Cu₃(BTC)₂. (Figure is reproduced from reference 34 with permission, Copyright, American Chemical Society, 2012).

Alkali (KOH or NaOH) treatment is one of the effective methods for activating porous carbon in order to enhance porous structure and pore widening which exerts superior electrochemical performance for example with high capacitance and excellent rate capability in both aqueous and non-aqueous electrolytes.⁴³⁻⁴⁵ This method can be more effective for the preparation of hierarchical porous carbon using non-templating route. A poly(vinylidene fluoride) (PVDF) derived porous carbon can be further improved by a two-step carbonization-activation process in which alkali (NaOH) acts as interceptor of HF and activation agent.⁴⁶ Such trick improves the percentage of meso- and macropores in the hierarchical interconnected network. With the increase of the concentration of NaOH activator, percentage of meso- and micropores increased and thus the pore volume with thinner pore walls with higher activation degree. This results a very high pore volume $2.28 \text{ cm}^3 \text{ g}^{-1}$ and BET surface area $2711 \text{ m}^2 \text{ g}^{-1}$. When compared between one-step activation with the two-step by NaOH, improved electrochemical performance recorded with the one-step activated material which reveals the efficiency of the former method and it perhaps due to the molten NaOH pored over the fresh surface of the micropores obtained

by the PVDF pyrolysis making a higher degree activation with increase in abundance of mesopores with a wider distribution in hierarchical interconnected pore network.

Activation of such polystyrene-derived HPC with KOH can give rise to unique 3D interconnected large meso- and macroporous structure (27.3 and 68.5 nm, respectively) among the carbon network.⁴⁷ High surface area of KOH activated PS-HPC ($3023 \text{ m}^2 \text{ g}^{-1}$) is even higher than that of the KOH activated order mesoporous carbon ($2060 \text{ m}^2 \text{ g}^{-1}$) however lower than that of the KOH activated polypyrrole-based carbons which possess irregularly shaped platelets or particle of larger size ($\sim 20 \text{ }\mu\text{m}$).⁴⁸ Specialty of this PS-HPC materials is that a large number of micropores and small mesopores whose pore size are large enough for ILs to access are formed within the carbon framework during KOH activation. This provides large interfaces for the formation of the electric double layer. An ideal non-templating strategy is therefore inexpensive to manufacture and easily sourced carbon; however, limited methods were reported which allows a huge scope for future.

4. Biopolymer Derived Porous Carbon

Application of biomaterials as biological template is known for nanostructuring of various inorganic materials and metal nanoparticles for which cellulose and polysaccharide nanocrystals play significant roles.⁴⁹⁻⁵¹ However, scope of accessing porous materials containing ordered well-defined pores from biomass was not explored until recently. As promising renewable resource, biomass offers attractive raw material and starch was already explored for the preparation of hierarchical porous carbons.⁵²⁻⁵⁴ Alginate, a naturally occurring polysaccharide extracted from marine brown algae, has attracted substantial attention for the applications in immobilization of enzymes and proteins and as template in fabricating nanostructured semiconductor materials.^{55,56} Alginate has abundant carboxyl and hydroxyl groups in its polymeric carbon matrix and it is particularly convenient as template in the aqueous phase due to the presence of negative charges of the glucuronic and mannuronic units.^{57,58} When all these functional groups have been converted to carbon oxides and water, the polymeric carbon matrix can be naturally converted to carbonaceous materials upon carbonization, turning alginate as suitable precursor for the fabrication of porous carbons.

The simplest approach to access porous materials from biomass is pyrolysis of native biomaterial under closed conditions or inert atmosphere. For potential applications like

supercapacitors, the uniformity of porosity in biomass would be most advantageous to obtain hierarchical porous carbon nanostructures derived from natural renewable resource making the strategy highly economical. In such case, the application of homogeneous biopolymer hydrogels or hydrothermal carbonization is essential. In addition to these, understanding the process of formation of hierarchical pore network in the carbon monolith obtained via carbonization is essential. Controlled carbonization of alginic acid fibers, prepared through a simple wet spinning method, offers a varied mesopores and micropores with different shapes and sizes around the nanoparticles that construct a hierarchical porous network.⁵⁹

Wet-spinning method offers preservation of regular and fiber-like shape of the alginic fibers which can be preserved after carbonizing with filaments exhibiting uniform 1D morphology with a diameter $\sim 10 \mu\text{m}$. Under higher magnification (Figure 6a), however, it is clear that the filament is composed of nanosized carbon particles (less than 10 nm) with a porous texture with no homogeneity in pore arrangements. Figure 6b shows morphology of a single filament, which exhibits a smooth surface both on the exterior and cross section of the filament under low magnification. Abundant interspaces around the nanoparticles revealed from the TEM image (Figure 6c) that carbon fibers are composed of an interconnecting 3D network of carbon particles and form a hierarchical porous structure composed of large mesopores ($\sim 19 \text{ nm}$ pore diameter) and abundant micropores ($< 2 \text{ nm}$). However, more essential is to understand the pathways of formation of hierarchical porous network from a controlled carbonization process of alginate framework of which oxygen might play a significant role in formation of graphenic carbon atoms as observed in the pyrolysis of alginate in presence of phosphorous source which offers a P-doped graphene.⁶⁰

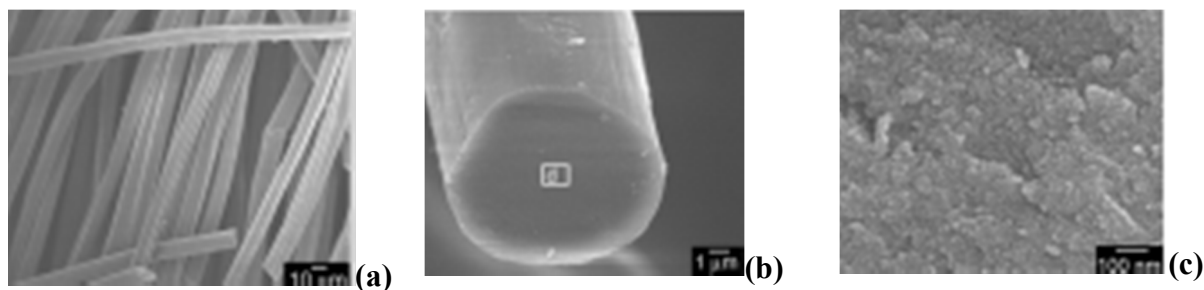


Figure 6. Typical SEM image of as-prepared HPCFs obtained from alginic acid fibers. a) regular fiber-like shape of alginic fibers after carbonization, b) morphology of a single filament with smooth surface both on exterior and cross section of the filament, c) under higher magnification,

filament is composed of nanosized carbon particles surrounded by fissures and hillocks with a unhomogeneously porous structure. (Published from the reference 16 with permission, Copyright Wiley-VCH, 2010).

Developing an efficient and facile synthesis protocol using the precursors accessible directly from natural sources for the preparation of 1D nanoporous carbon with well-tailored architectures would be of great significance. Toward this direction, it is demonstrated that an electrospun fiber-like natural cocoon microfibers can be directly transformed into 1D carbon microfibers with an average diameter of 6 μm . The most relevant fundamental question would be how a unique 3D porous network, consisting of 1D carbon microfibers built with numerous carbon nanoparticles (10-40 nm), was obtained via a carbonization (Figure 7).⁶¹ The recipe of the network of hierarchical porous structure is that these carbon nanoparticle contain microporous and their compact and loose aggregation leads to the formation of mesopores and macropores, respectively. Interlacement of 1D carbon microfibers themselves in the carbonized cocoon leads to formation of large macropores. Due to effective pore interconnectivity, high surface area, large pore volume as well as high nitrogen content, as-prepared 1D HPC microfibers (HPCMF) exhibit superior electrochemical performance as binder-free electrodes of supercapacitors and promising adsorption behavior for organic vapor.

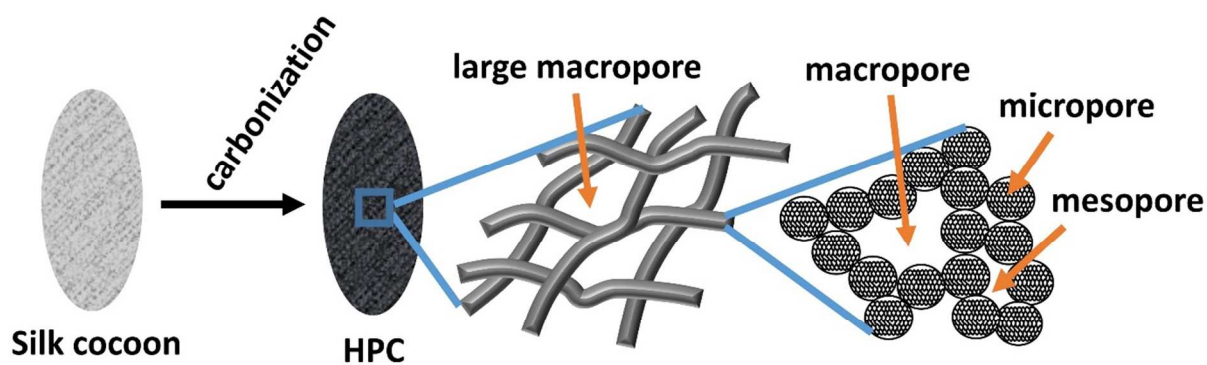


Figure 7. Silk cocoon as source of hierarchical carbon

Biomass-derived porous carbons, such as from fungi,⁶² corn grain, lignocellulosic materials,⁶³ fish scales,⁶⁴ starch,⁶⁵ celtsuce leaves⁶⁶ were already reported. These showed great potential as electrode materials for supercapacitors or as solid adsorbents for CO₂ capture. In

such pyrolysis methods, by optimizing the carbonization temperature, porosity and capacitance of the resulting porous carbon can be balanced. For example, porous activated carbon derived from celtuce leaves (CL) by air-drying and pyrolysis offers a continuous and distorted layered microstructure which can facilitate the KOH impregnation and activation (Figure 8). Indeed nanoscale pores and local curvature was formed in as-prepared carbon due to the KOH etching of CL and generate a substantial micro/mesopores of extremely small size (0.5 to 5 nm) and large mesopores and/or the textural macropores (30 to 60 nm) with interconnectivity that are homogeneously distributed throughout the porous structure.

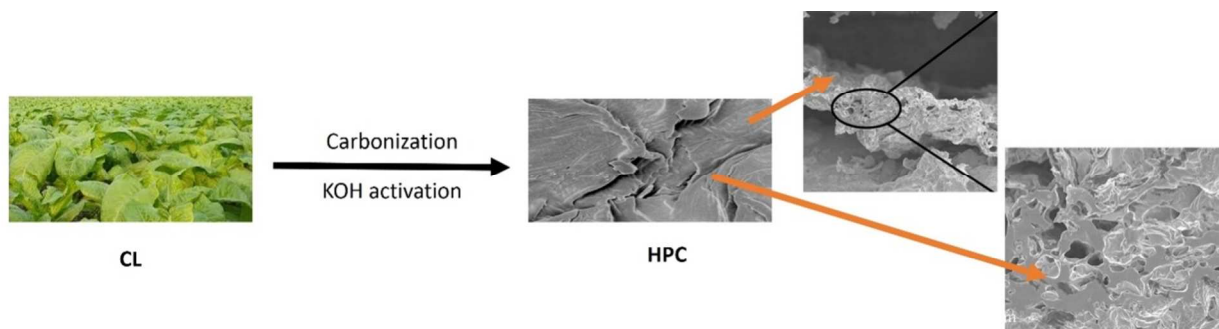


Figure 8. Carbonated celtuce leaves surface morphology and cross-section morphology showing the pore network.

Alkali (KOH or NaOH) treatment can also be used as effective strategy for constructing or improving hierarchical pore network in the biomass-derived porous carbon as demonstrated for HPC microspheres derived from porous starch.⁶⁷ In this case, the KOH activation of the carbon microspheres resulted a new porous structure on the surface of the ladder-like channel (Figure 9(f)). The pores created by KOH along with the macropores inherited from the precursor offers a 3D hierarchical structure with incredibly high BET surface area $3251 \text{ m}^2\text{g}^{-1}$. Most of the macropores were inherited from the precursor. There are four main regions, including the ultrafine 0.4-0.7 nm and 0.9-1.3 nm micropore region. The 4-14 μm pores in the starch precursor contributes more to the total volume of HPC microspheres. The predominant pore size in HPC microspheres is in the range of 0.7–4 μm which is likely due to shrinkage during the carbonization.

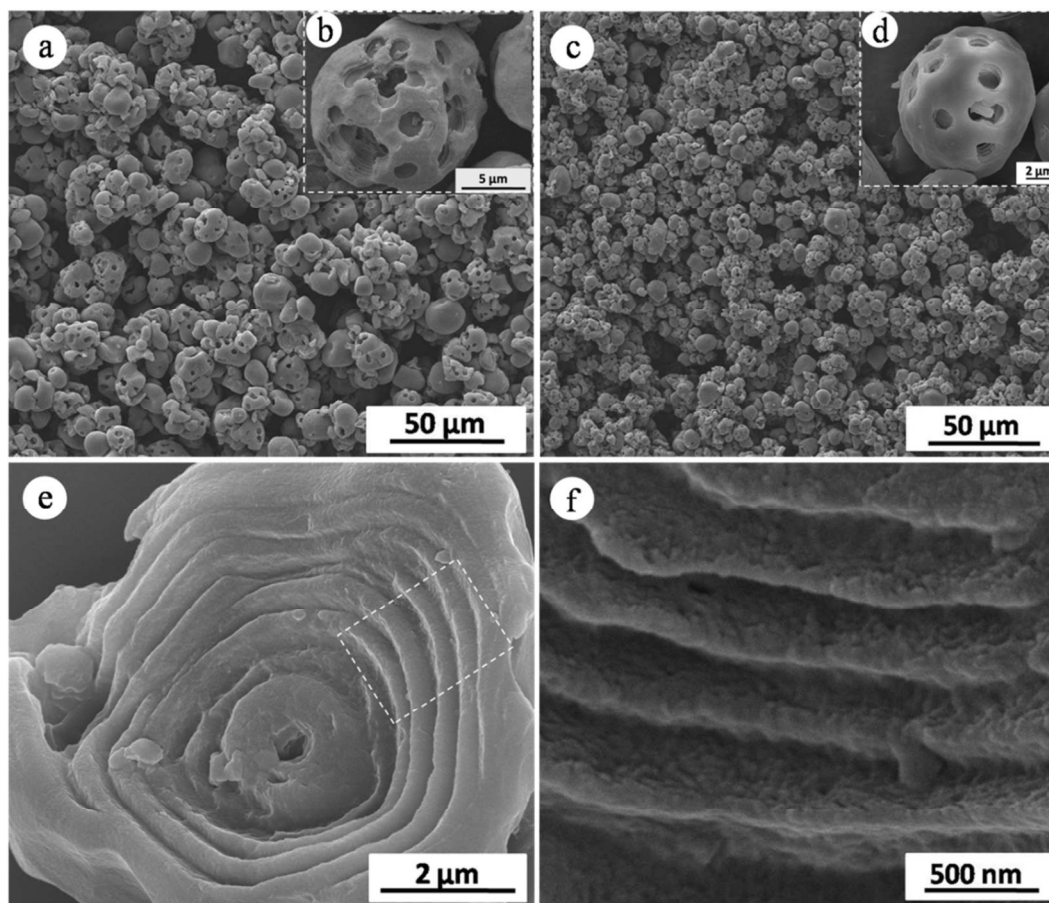


Figure 9. The SEM images of (a) the porous starch precursor, (b) a porous starch granule under high magnification, (c) the hierarchical porous carbon microspheres, (d) the hierarchical porous carbon microspheres under high magnification, (e) the internal ladder-like microstructure of the hierarchical porous carbon microspheres and (f) the selected part in (e) under high magnification.

Natural cellulose substance such as filter paper and cotton possess a macro to nanoscopic random morphological hierarchy consisted of β -D-glucose chains. Replication of this sophisticated network at nanometer level was realized previously by coating ultrathin metal oxide gel films on each cellulose nanofiber surface via the surface sol-gel process.⁶⁸ Stable suspensions of nanocrystalline cellulose (NCC) can be obtained through hydrolysis of bulk cellulosic material with sulfuric acid. In water, suspensions of NCC organize into a chiral nematic phase that can be preserved upon slow evaporation, thereby resulting in chiral nematic films.^{69,70} NCC–silica composite films may also be used to generate mesoporous carbon (MC) with a high specific surface area and excellent chiral nematic organization (Figure 10).⁷¹ Though

soft-templating is more promising strategy, however, while using NCC as structural template, use of mesoporous silica is essential for mesoporosity and preservation of the long-range chiral organization. This is due to the formation of linkages between the carbon regions during pyrolysis which may be prevented without using silica or using higher silica loading and formation of thicker silica walls. At an optimum silica concentration, maximum BET surface are ($1465 \text{ m}^2 \text{ g}^{-1}$) and micropore volume ($1.22 \text{ cm}^3 \text{ g}^{-1}$) can be achieved. Chiral nematic mesoporous carbon (CMC) also exhibits locally aligned pores originated from local nematic organization. This CMC films contain smooth surfaces with a repeating layered structure perpendicular to the surface. Apart from the great possibility of CMC materials as hard-template capable of transferring chiral nematic structure to the other material, this also displays semiconducting property which increases in raising temperature.

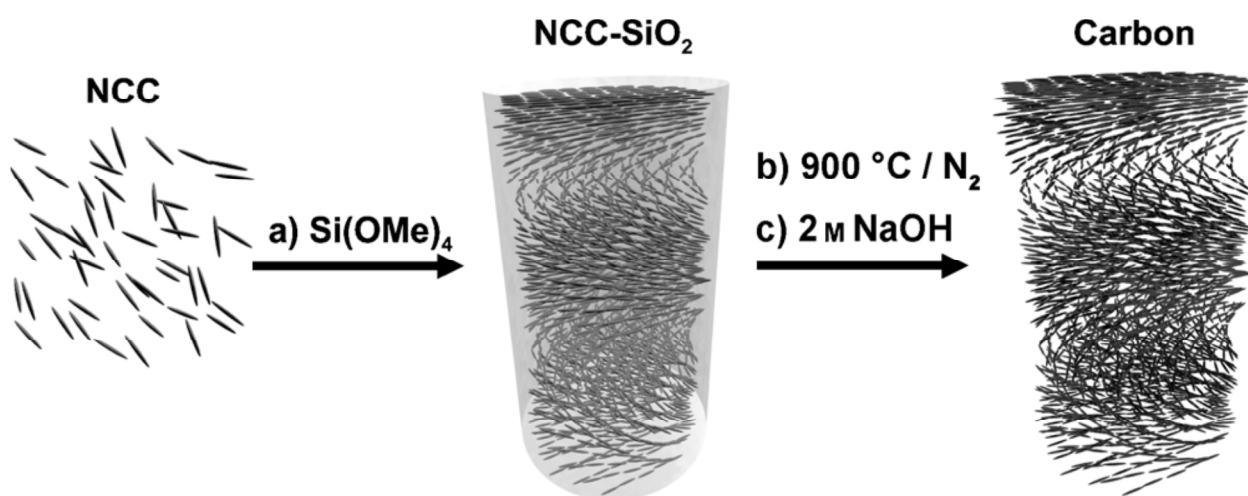


Figure 10. Chiral nematic porous carbon via NCC-silica composite films, pyrolysis at 900 °C, and silica removal from carbon-silica composite.

As a promising resource of nanochemistry, biomass-derived materials have several advantages. They are naturally abundant and many are extracted industrially on a large scale as low-value waste products. For example, lignin from kraft pulping. Currently new approaches for utilizing biomass-derived cellulose as source of HPC and other new materials has been witnessed, however, in the near future, we hope to see both extracted biopolymers and native biomass will be explored.

5. Hetero-Atom Doped Porous Carbon Monolith

The incorporation of heteroatoms, such as B, N, P and O, into the carbon lattice can significantly enhance the mechanical, semiconducting, field-emission, and electrical properties of carbon materials.⁷² These heteroatoms in the porous carbon may enhance the electrical conductivity, influence the wettability, or consequently maximize the electroactive surface area.⁷³⁻⁷⁶ Recent studies suggest that surface functional groups or doped heteroatoms play important roles in improving the performances of the carbonelectrodes.⁷⁷⁻⁷⁹ Doping carbon materials with electron rich atoms has its own advantages for advanced technological applications. Such strategy become even blissful when the biomass-derived proteins serve as precursor for synthesizing carbon materials with unique structure, high specific surface area ($805.7 \text{ m}^2 \text{ g}^{-1}$), partial graphitization, and very high bulk nitrogen content (10.1 wt%). However, this above method depends on the templating strategy of egg white-derived protein to template the structure of mesoporous cellular foam.⁷⁶ Current carbon supercapacitors have extensively used redox reactions to increase their charge-storage capacity. Redox reactions associated with oxygen-containing phenol or quinone/hydroquinone scan contribute one electron; phosphorus atoms which stabilize oxygen functional groups during electrochemical charging and gas-phase catalysis. This improves reaction stability and selectivity.^{80,81} Boron atoms in a carbon lattice are able to promote the chemisorption of oxygen for a more-reactive carbon surface.⁸² The advantage of nitrogen doping to the porous carbon surface would cause a shift of the Fermi level to the valence band in carbon electrode that would be essential for the supercapacitor applications. The combined effect of nitrogen/oxygen-containing functional groups was also evident in capacitance-enhancement.⁷³

Two methods are commonly used to prepare nitrogen-rich carbon materials. One is the simple heat treatment of nitrogen-containing precursors (such as melamine-based polymer, polyacrylonitrile, vinylpyridine resin, and silk fibroin) under an inert atmosphere.⁸³⁻⁸⁵ The other method is the low-temperature treatment ($250\text{-}350 \text{ }^\circ\text{C}$) of carbon materials in a mixture of ammonia and air with different volume ratios.⁸⁶ Location of the N-centers of the carbon lattice of porous carbon monolith which contributes to the efficiency of the materials for supercapacitor and gas adsorption applications. Generally, HPC obtained from the carbonization of nitrogen-containing precursors offers more quaternary nitrogen centers (N-Q) (located at the center and valley position of carbon lattice) which lacks in ammonia-assisted carbonization method.

Ammonia-assisted carbonization of thermosetting-type phenolic resin obtained via magnesium hydroxide templating offers a significant nitrogen doping in carbon which increased the surface area with the involvement of different nitrogen groups for the ion transport and also depends on the relative redox activities of the nitrogen groups.⁸⁷ In the case of magnesium hydroxide templating, heat treatment in ammonia resulted an unexpected increase of the BET specific surface area and micropore volume. This happens due to edge-nitrogen atoms connected with two carbon atoms which motif prevented the growth of the carbon lattice, leaving more space as micropores. Generation of micropores or the expansion of the micropores occurs due to the release of hydrogens which etch carbons that causes removal of carbon atoms from lattice.

The CO₂ adsorption capacities of nitrogen-rich porous carbons have been less studied as compared with amine-functionalized porous silica. As compared to commercially available activated carbons, polymer-based synthetic porous carbons have high purity, good reproducibility, and well-defined pore structures. Thus, such porous carbons have also been modified to nitrogen-rich porous carbons by deliberate selection of N-containing carbon precursors, such as melamine. For instance, highly nitrogen-enriched porous carbons were prepared from melamine–formaldehyde resins.⁸⁸ Recently, various nitrogen-containing porous carbon monoliths were fabricated and used for CO₂ capture and separation.⁸⁹ Using resorcinol–formaldehyde as carbon precursors and the amino acid l-lysine as the catalyst, a type of nitrogen-doped porous carbon monolith was synthesized by Lu and co-workers which possesses maximum CO₂ capture capacity 3.13 mmol g⁻¹ at 25 °C and 1 atm under a flow of pure CO₂.⁸¹ Subsequently, a nitrogen-containing porous carbon monolith with fully interconnected macroporosity and mesoporosity was fabricated which withstand a pressure of up to 15.6 MPa.^{88,90}

To avoid using harsh chemicals for activation and sacrificial templates, physical activation to obtain activated carbon materials is highly desirable from both environmental and economic points of view. The CO₂ uptake capacity can be enhanced by incorporating basic N-functional groups and narrow micropores (< 1 nm) with high adsorption potential. A porous activated carbon monoliths (ACMs) can be accessed via activation-carbonization of mesoporous polyacrylonitrile (PAN) monoliths in an oxidizing CO₂ environment (Figure 11).⁹¹ The formation of carbon with a lamellar phase occurred by carbonization of rigid polymer with extended 2D-framework obtained from the PAN monolith via the cyclization inside the polymer

framework. Cyclization-aromatization imparts extra rigidity to the polymer network which may be responsible for the creation of narrow micropores. During carbonization, removal of nitrogen from the framework causes fusion of the molecular ladders which results in extended sheet-like lamellar carbon frameworks. Micropores randomly distributed all over the skeleton of the microstructures and N-rich porous surface are held responsible for CO₂ uptake with maximum 11.51 mmol g⁻¹ at 273 K.

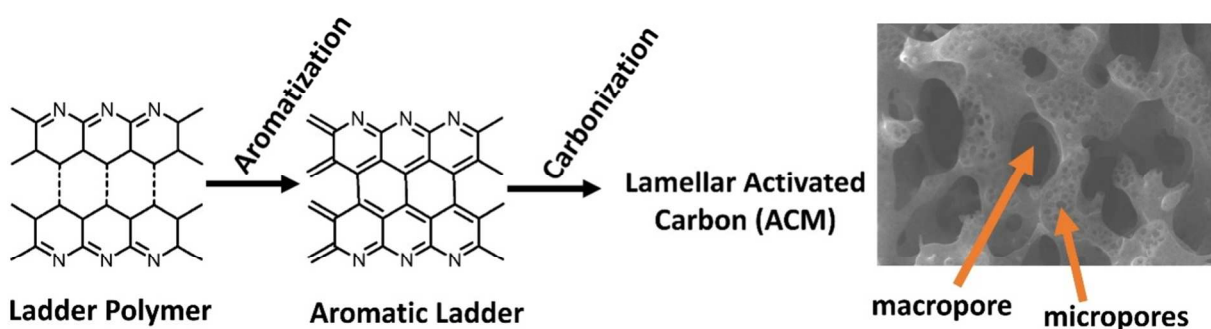


Figure 11. Formation path of ACMs with narrow micropores in the carbon framework.

Phosphate-functionalized carbon materials are interesting because of the widening of the operational voltage window with aqueous electrolytes and the subsequent increase of the energy that can be attained. A resorcinol-based deep-eutectic solvents (DESs) composed of resorcinol, choline chloride, and glycerol assisted synthesis of phosphate-functionalized carbon monoliths (PFCMs) via the polycondensation of formaldehyde in the presence of phosphoric acid as catalysts can give access to a bicontinuous porous network built with highly cross-linked clusters that are aggregated and assembled into a stiff, interconnected structure.^{84,85} Bi-continuous (micropores and mesopores) structures contains macropores of 0.56 μm resulting from the spinodal decomposition process at the resorcinol polycondensation stage in which a polymer-rich phase may form with the segregation of the non-condensed matter. The DES-assisted synthesis offers hierarchical porosity in phosphate functionalized carbon monolith with direct assembly of carbon cylinders excellent for supercapacitor electrodes. In this process, DES plays multiple roles such as tailoring the textural properties and composition of resulting carbon materials as a structure directing agent and carbonaceous precursor. Moreover, the template effect of DESs was reflected in HPC monoliths with maximum pore surface areas 600 m²g⁻¹ and narrow mesopore diameter distributions.

N and B co-doped carbon monolith with hierarchical pores can be accessible via self-assembly-carbonization process starting from poly(benzoxazine-co-resol) and ionic liquid [C₁₆mim][BF₄] as carbon and boron source respectively.⁹⁴ A high skeleton density and fully interconnected pore network with ultramicropores (pore width < 1 nm) was obtained. This pores are suitable for the diffusion of electrolyte ions by minimizing the molecular diffusion limitations, thus potentially advantageous for enhancement of supercapacitor performance. The nanostructure of the carbon-boron co-doped carbon (CNB) contains a random combination of graphitic and turbostratic stacking with short range ordering and displays a graphite-like microstructure with good electrical conductivity due to the multi-length-connected carbon framework. The electron conductivity in the carbon materials is enhanced due to the redistribution of π electrons in the presence of substituted boron and nitrogen that weakens C–C bonds and strengthens C–O bonds when exposed to air. Ionic liquid plays a role of introducing heteroatoms into the carbon framework through particle involvement in the condensation process.

From the above discussion, it is revealed that for improved conductivity of ions for a range of applications such as supercapacitor, introduction of heteroatoms in the local graphitic carbon matrix is essential. Multiple heteroatom incorporation into a carbon matrix is comparatively a new strategy to enhance electron conductivity for electrochemical energy storage applications. This strategy depends on the molecular design of monomers and choice of solvent/media which is capable of supplying heteroatoms to the carbon matrix during the condensation process. Simultaneous control of nanoporosity and electrochemical accessibility of the nitrogen atoms are essential for nitrogen-enriched nanoporous carbons and a general synthetic pathway is desired. However, most frequently used strategy so far is the use of well-defined block copolymers as precursor for nitrogen-enriched carbon and sacrificial block serves as a source of mesoporosity.

6. Synergistic Effect of Macro-Meso-Micropores for Applications

Compared to conventional porous materials consisting of uniform pore dimensions that can be adjusted over a wide range of length scales, hierarchical porous materials with well-defined pore dimensions and topologies can exhibit minimized diffusive resistance to mass transport from macropores and high surface area for active site dispersion from micro- and/or mesopores.

Depending on the specific requirement of many emerging applications related to energy storage, environmental cleaning, and sensing, hierarchical nanoarchitecture of the carbon materials is essential. A number of emerging applications of carbon materials is identified and how the hierarchical interconnecting porous network is desired are discussed here in.

6.1 CO₂ Storage Materials

Development of new porous materials as sorbents for CO₂ removal via selective adsorption find potential applications in flue gas treatment and natural gas upgrading which are considered as clean energy technologies. This captured CO₂ can further be used as feedstock to produce liquid fuels or can be offered to microbes that consume CO₂ and produces fuels. Carbon capture and sequestration in the form of CO₂ adsorption is a coherent extension of solar-to-fuel and biomass conversions to biofuels. For the capture of CO₂ from flue gas mixtures the materials are usually operated under ambient conditions. Thus, gas diffusion properties become the dominant factor which indicates balance among the surface area, pore size and interconnected pore structures. Generally, a highly porous adsorbents when doped with nitrogen⁹ or in monolithic form under relatively mild conditions would facilitate large-scale applications. The reversible absorption/desorption based on the humidity swing is very similar to the green leaf that displays net CO₂ uptake in sunlight and output in dark in which a functional porous material would act as the “artificial leaf” that is able to capture and release CO₂ in ambient air under dry and wet conditions, respectively.⁹⁵ The porous support materials consist of immobilized quaternary ammonium cations with hydroxide, bicarbonate, or carbonate counter anions would be desired materials under dry and humid conditions.⁹⁶ Materials with high specific surface areas generally contain a large number of micro- and mesopores, which may decrease the kinetics of absorption and desorption due to diffusional limitations. Additionally, the capillary forces in the micropores can also decrease the sorption rates. It would be highly desirable to obtain porous carbon materials accessible from the macroporous polymers for the reversible CO₂ capture under ambient air by humidity swing with an improved absorption/desorption kinetics controlled by the hierarchical porous framework. Given that the recent studies show both high porosity and interconnectivity between pores makes a material best performing and such material can be obtained via sacrificial templating. Functional material of same porosity can be accessible from suitable carbon source which retain the structure of the template upon carbonization.

For CO₂ capture and storage, the inclusion of analogues of water soluble amines into the walls of solid porous materials and the construction of nitrogen-rich porous adsorbents provide several advantages as compared with the costly regeneration step in the amine-based solution absorption process. A nitrogen-rich porous carbon with a hierarchical micro/mesoporous structure exhibiting fast adsorption-desorption kinetics is highly desirable.¹³ Nitrogen-rich porous carbons open the door for the preparation of highly effective carbonaceous adsorbents for CO₂ capture. The relatively low synthetic cost and easy fabrication, combined with an excellent efficiency of CO₂ adsorption and separation, make nitrogen rich porous carbons highly promising for CO₂-selective adsorption in practical applications. Porphyrin based nitrogen rich porous organic polymers (POPs) are another interesting candidate for CO₂ capture from flue gas.⁹⁷ A wide range of POPs can be synthesized through extended aromatic substitution involving the condensation of pyrrole with aromatic dialdehydes in the presence of Lewis acid FeCl₃ under solvothermal conditions. High surface area and N-rich polymeric network together with porosity facilitates their large CO₂ capture. It has been observed that ordered 3D-hexagonal mesoporous silica HMS-4 functionalized with vinyl groups at the surface of the mesopores could adsorb 5.5 mmol g⁻¹ (24.3 wt%) under 3 bar pressure at 273 K⁹⁸ due to its cage like pore openings, very high surface area and organic functionalization over related mesoporous silica-based materials.

6.2 Carbon Photonic Crystals as Sensors

It has been observed that the glassy carbon nanostructures obtained via porous silicon templating function as highly efficient adsorbents for volatile organics and also act as optical vapor sensors.⁷ This photonic properties of the carbon-infiltrated composite pSi film was found to be amended than the Si-based sensor and sensing strength depend on the porous nature of the surface containing two different types of mesopores. Upon removal of Si-template, porous carbon membrane can be retained when immersed in liquid (methanol, ethanol, hexane, toluene) and this act as photonic crystals. From highly porous carbon replicas with extremely high structural fidelity in silicon template, a carbon nanofiber arrays can be obtained. This carbon nanofiber material in liquid media would be a better alternative as photonic sensors. The similar material can also be used for the adsorption/desorption phenomena. The enhancement of refractive index of pore interior for the red-shifting of the position of the photonic stop band is essential criteria.

Thus a porous layer of carbon would act as organic toolkit to the silicon surface since carbon is superior adsorbent which uniformly cover Si layer.

6.3 Li-S Batteries

Li-S battery considered to hold great potential for the next generation of large-scale and high energy density energy-storage devices. In order to tackle the problem of high solubility of intermediate soluble polysulfide ions which results in a shuttle phenomenon between anode and cathode and loss of active mass, carbon materials with hierarchical pore structure can encapsulate and sequester elemental sulfur for high-performance Li-S batteries. This improves electrical conductivity and prevents polysulfide dissolution.⁹⁹ It was found that HPCs with mesoporous walls and interconnected macropores encapsulates element that results improvement in performance of Li-S batteries. Contribution of mesopores in encapsulation of sulfur suggests the presence of hierarchically ordered structure.¹⁰⁰ This materials walls are composed of spherical mesopores, which indicates a hierarchically ordered porous structure in which elemental sulfur could be impregnated into the mesoporous walls of HPC in a highly dispersed state, which inhibit aggregation of sulfur and initiate essential electrical contact. The mesopores while serving as container, traps elemental sulfur and subsequent lithium polysulfides during charge/discharge process. In this process, an appropriate ratio of mesopores/macropores facilitates the transition of Li^+ during electrochemical cycling by reducing the ionic and electronic conduction distance. Thus integration of mesopores (sulfur lithiation) and macropores (ion transport) would be an essential feature for the next generation hierarchically porous carbon materials for Li-S battery applications.

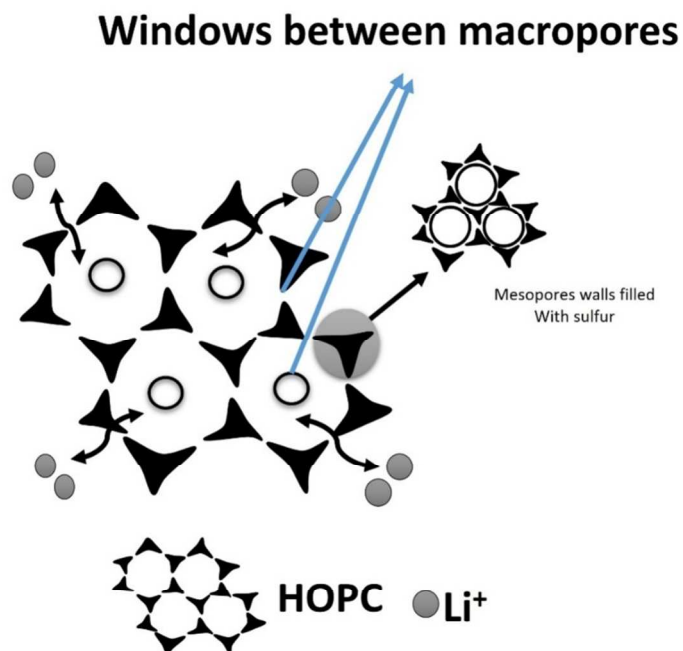


Figure 12. The electrochemical reaction process inside the pores of HOPC/S nanocomposite cathode.

6.4 Supercapacitor

Effective utilization of intermittent renewable sources facilitates energy storage and electrochemical energy is stored in supercapacitor to transport high power within a short period in a portable electronic devices and hybrid electric vehicle. Development of electrode having both high end a specific capacitance, closely related to the availability of interconnected meso-micropores and high rate capability. A hierarchical structure with well-interconnected small and large pore would provide opportunity to optimize the specific capacitance and rate capability of carbon materials as supercapacitor electrode. In general, since SC stores energy physically at the electrode/electrolyte interface based on electrochemical double-layer mechanism for which high surface area is the basic requirement in carbon-based electrode materials. However, for commercial porous carbon, poor rate performance is used to be observed due to the low conductivity, high ion-transport resistance and insufficient ionic diffusion within the tortuous micropores, which limits its application in the high-power energy storage devices. What is missing in this commercially available carbon is additional second-order structure of

meso/macropores which needs to be induced. Three-dimensional (3D) porous nanostructure is desirable for high-performance electrode materials. The 3D nanoscaled architecture can not only provide a continuous electron pathway to ensure good electrical contact, but also facilitate ion transport by shortening diffusion pathways. The superior electrochemical performance of the carbon is attributed to its unique hierarchical porous structure, which provides the critical features required for advanced supercapacitors: the abundant micropores and mesopores provide the electrode with a high accessible surface area, resulting in a large capacitance and high energy density, while interconnected mesopores and macropores facilitate ion transport, which ensure high rate capability and high power density.¹⁰¹ Hierarchical porous carbon (HPC) materials have elicited porous structures are able to exhibit the advantages of each pore size with a synergistic effect during electrochemical charge-discharge process. Macro/mesopores facilitate rapid ion transport by serving as ion-buffering reservoirs and ion-transport pathways,^{12(d),13} and the micropores enhance the electrical double layer.^{102,103} Porous carbon materials when used as electrode in electrochemical capacitors, suffers from electrode kinetic problems which is due to the inner-pore ion transport resulting poor performance.^{102,104} In spite of the fast ion transport ability as well as the high utilization of surface area, HPCs still suffer from a low energy density, a universal bottleneck for electric double-layer capacitors (EDLCs).

6.4.1 Mechanism of Ion Transport and Buffering

The exact mechanism of ion transport within porous materials is highly complex for which various factors such as shape of pores, connectivity, pore-size distribution should be considered. Apart from the pore structure and shape, nature of electrolyte and solid-liquid interface must all be considered. Among these factors, the inner-pore ion transport resistance and diffusion distance are the most important factors. Generally, micropores ($d < 2$ nm) exhibit large specific surface areas but ion transportation may be interfered by pore walls resulting poorer power density. When the pore diameters are smaller than solvated ions, the formation of double layer is supposed to be impossible. However, in certain cases electric double layer is formed even when the solvated ions are larger than pore diameters when using an organic electrolyte (LiClO_4 in propylene carbonate and dimethoxy ethane).¹⁰⁵ In hierarchical porous structure, electrolyte ions can be delivered smoothly through meso/macropores to micropore surfaces with large specific surface areas. From the fundamental viewpoint, analysis of contribution of capacitance by meso/macropores and micropores, separately is essential, however, in the case of porous carbon,

pore sizes are continuously distributed from micropores to mesopores, thus makes the analysis complicated. In addition, electrolyte transport in their narrow pores cause the kinetic polarization and thus capacitance may be underestimated. It is believed that pores substantially larger than the size of the electrolyte ion and its solvation shell are required for high capacitance. The demonstration of charge storage in pores smaller than the size of solvated electrolyte ions will lead to enhanced understanding of ionic transport in porous media. These findings should also permit the design of application specific supercapacitor for longer discharge times where energy density is at a premium, such as in hybrid electric vehicles, extremely narrow pores should prove optimal, but for pulse power applications, increasing the pore size might be beneficial.

6.4.2 Electrical Double Layer Enhancement

In the case of ordered mesoporous materials, interconnectivity of channels is beneficial in improving ion diffusion properties. An efficient pore network and interconnectivity of channels can lead to much lower impedance to ion transport within both the channels and the micropores in the carbon wall, and thus has better electric double layer performance. Doping with electron deficient element (*e.g.* B) with valence electrons, can introduce a hole charge carrier once it replaces a carbon atom in the carbon lattice. This would increase the charge density and further improve the double layer capacitance. This doping also improves the polarity of a carbon matrix by improving the wettability, and allow an easy diffusion of the electrolyte ions into micropores. The local graphitic heteroatom-incorporated carbon matrix presents a higher conductivity due to their exceptional nanostructure and surface characteristics. According to Largeot et al. 2008, when the pore size of the electrode materials is close to the size of ion in the electrolyte, a maximum capacitance can be obtained.¹⁰⁶ Taking into account the fact that the solvated ion size of K^+ is between 0.36 nm and 0.42 nm, it can be predicted that the pores of these first two regions will contribute the most to the formation of the electric double-layer, leading to a high capacitance as described by Eliad et al.¹⁰⁷ The other two regions are the 1.3-3.4 nm micro/mesopore region, which plays a role in electrolyte ion diffusion paths and the >50 nm macropore region, which serves as ion-buffering reservoirs and thus decrease the ion transport distance during electrochemical processes for a starch-derived hierarchical carbon. Contribution of meso/macro and micropores to C_{DL} can be analyzed by the following equation.

$C_{DL} = c_{dl,meso}S_{meso} + c_{dl,micro}S_{micro}$ where $c_{dl,meso}$ and $c_{dl,micro}$ are specific electric double layer capacitance on meso/macropores and micropores respectively. Here ion sieving effect of micropores comes into play in the case of using electrolytes with positive ion radius slightly larger than the micropore radius.¹⁰⁵

6.4.3 Ion Diffusion

Unique hierarchical porous structure of the HPCs that favors the rapid diffusion of electrolyte ions into the pores in a supercapacitor electrodes. In a hierarchical porous architecture, large mesopores would provide fast diffusion channel for electrolyte and the diffusion distance would also be very short owing to that the micropores were located within the mesopore wall. Micropores are expected to be the most efficient in a double-layer formation. The energy and power limitations normally observed at high rates are associated with the complex resistance and the tortuous diffusion pathways within the porous textures. At high discharge current, only some parts of the pores (mainly the outer regions) can be accessed by ions, whereas at low current, both the outer- and the inner-pore surfaces are used for charge storage. The good energy and power performances of HPCs confirm that most of micropores within the mesoporous skeleton can be effectively utilized for charge storage. A reduced capacitance of microporous carbons at large discharging current densities was found; however, such reduced capacitance also exists for mesoporous carbon materials, probably because of the solute diffusion process.

7. HPC versus Ordered Mesoporous Carbon (OMC)

The links between the hierarchically porous structure and their role in performing energy conversion and storage can promote the design of the novel nanostructures with advanced properties. Apart from providing large surface areas, HPCs can provide interfacial transport, dispersion of active sites at different length scales of pores (macro, meso, micro), and shorter diffusion path. Some theoretical calculations predict that the hierarchically macro-, meso-, microporous structured catalysts can reduce the diffusion limitations.^{108,109} Low resistance and short diffusion pathway facilitate fast electron and mass transport to enhance the electrochemical energy storage performance.¹¹⁰ HPCs exhibit outstanding behavior in diffusion-assisted adsorption applications driven by the different ranges of interconnected pores. This is very different from the ordered mesoporous network which provides shorter diffusion pathways along

the carbon particles, which enhances the diffusivity of molecules and/or ions. Generally, while construction process of HPCs, removal of hard-templates and carbonization of carbon source material results microporosity in the resulting carbon and mesoporous network generates as a result of incomplete pore filling of the hard template.

Ordered mesoporous carbons (OMC) received considerable attention owing to their large surface area, tunable pore structure, uniform and adjustable pore size, mechanical stability and good conductivity. In spite of containing these outstanding features, most of the mesoporous carbons derived so far have highly hydrophobic surface and a limited number of specific active sites, which impedes their practical application. The synthesis of HPC and OMCs depends on several factors such choice of C-containing precursor or N source for N-doped porous carbon. For example, directly self-assembly of organic-organic amphiphilic block copolymers has been a versatile route to access OMCs, however these strategy suffers from inferior pore structure with poor thermal stability or low N content. The reason behind the collapse of mesostructure is the pluronic surfactant with high oxygen content which promotes decomposition of N-containing part of the precursor. In addition, pyrolysis at high temperature can also accelerate the decomposition of the frameworks, resulting in collapsed mesostructure. When a direct synthesis of ordered mesoporous carbons from organic-organic self-assembly with high doped element (e.g. N) suffers from high N content and large surface area is a great challenge and in most cases direct carbonization offers material with wide pore size and disordered mesostructure.¹¹¹

Hao et al. reported the direct self-assembly of poly(benzoxazine-co-resol) followed by a carbonization process, obtaining N-doped porous carbons with well-defined hierarchical porosities⁸⁸ that contains defined multiple-length-scale pore structures (macro-, meso-, and micropores) of fully interconnected macroporosity and mesoposity with cubic $Im3m$ symmetry. This offers a remarkable mechanical strength to the material. The generation of highly interconnected pores in the nanostructures is dependent on the self-assembly of poly(benzoxazine-co-resol) and carbonization process. In this process, polybenzoxazine segments form hydrogen bonds (Ar-O-H...O) with the EO segment of F127 to a significant extent, which guide the mesostructure assembly within polymer species and the amphiphilic copolymer template (F127). During the following curing step, the unreacted resorcinol and formaldehyde would copolymerize with polybenzoxazine. In this case, both the polybenzoxazine

and poly(resorcinol-formaldehyde) together form the hybrid skeletons which leads to the formation of stable mesostructures.

In case of OMCs, N source is external while thermosetting polymerization, N source is incorporated. However, in the case of using polybenzoxazine-co-resol self-assembly in the presence of F127, N-source is attached with the copolymer undergoing the self-assembly before the carbonization. The difference is using resorcinol-dicyandiamide one would obtain ordered mesoporous framework and other provides porous framework with interconnected multi-length-scale pore structure via a copolymer self-assembly when using polybenzoxazine-co-resol. Controlled experiments revealed that mesopores has been generated via the assembly of polybenzoxazine and the ethylene oxide (EO) segment of the F127 due to the oxygen affinity of the O centers. It reveals that the presence of surfactant F127 is essential for the mesopores formation. Further, the condensation of the resorcinol with the polybenzoxazine and assembly of the resorcinol segment of the poly(benzoxazine-co-resol) with the EO segment offers the hierarchical pore formation. While using a resol-based copolymer such as poly(benzoxazine-co-resol) with F127 as template, two segments (benzoxazine and resol) separately interacts with the F127's EO segment via H-bonding and electrostatic interactions, and this a more complex self-assembly forms in solution which upon evaporation of solvent and pyrolysis produces interconnected pore networks in the nanostructure (Figure 13).¹¹¹ From this comparative study on the synthesis of OMC and HPCs, it reveals that the carbon source polymer played a crucial role in determining the nanostructure of the porous carbon when using the same polymer template with oxygen containing blocks.

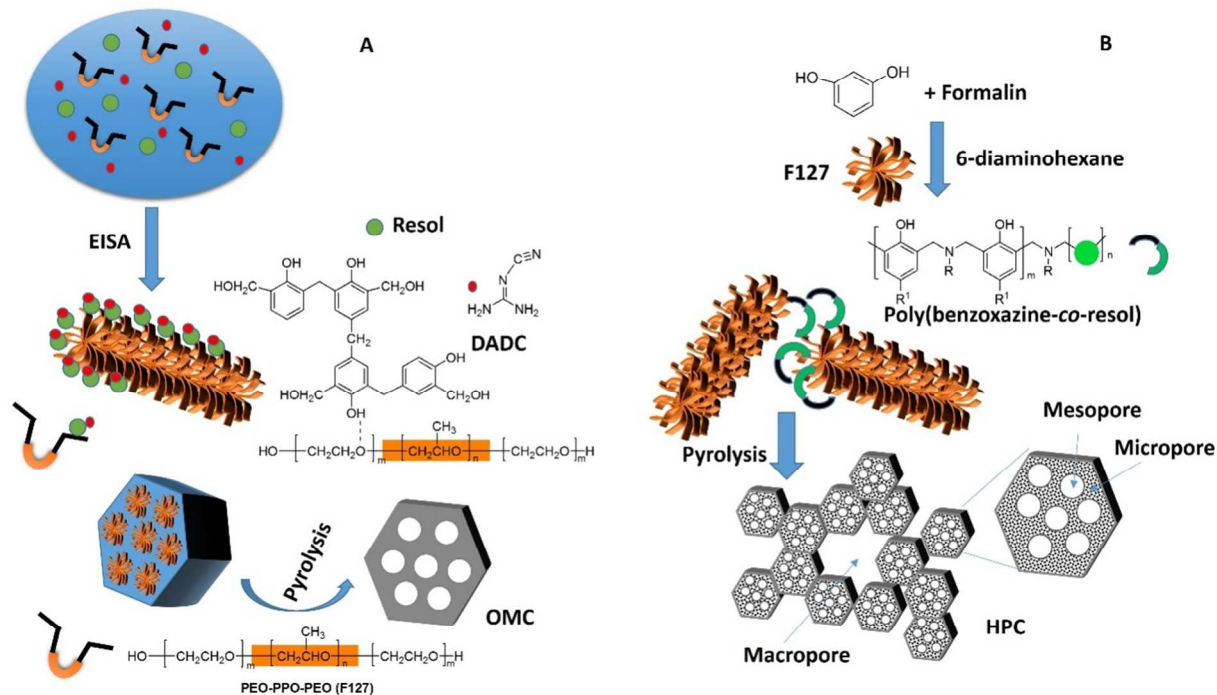


Figure 13. Formation of HPC and OMC by using F127 as soft-templates, where the resol and polymers are being used as the carbon sources.

Ordered mesoporous structures are slightly degenerated which is revealed from the small-angle X-ray direction (SAXS) patterns of $P6m$ 2D hexagonal mesostructure of H-NMC obtained various mass ratio of dicyandiamide (DCDA) to resol. In this material, uniform mesopores are periodically aligned over a large domain as revealed from the cross-sectional field-emission scanning electron microscope (FESEM) analysis.¹¹²

Unique nanoscale spherical OMCs with extremely high bimodal porosities are attractive material for applications involving rapid charge discharge capacity and good recyclability. A two-step nanocasting process to obtain spherical mesoporous carbon nanoparticle with hierarchical pores involves application of silica inverse opal which was used as template for a triconstituent precursor solution containing resol, tetraethylorthosilicate (TEOS), Pluronic F127 as structure directing agent.¹¹³ This process involves carbonization and etching of silica inverse opal template results OMC with hierarchical porosity. In this case, silica inverse opal templating creates OMC with high inner pore volume ($2.32 \text{ cm}^3 \text{ g}^{-1}$) with very high surface area ($2445 \text{ m}^2 \text{ g}^{-1}$) and a bimodal pore size distribution with bimodal pore size distribution of large and small

mesopores of 6 nm and 3.1 nm. Bimodal pore size distribution arises from the porous walls formed by etching the silica from the carbon/silica nanocomposite walls.

8. Future Potentials of HPCs in Emerging Nanotechnologies

Hierarchical pore arrangement of HPC has placed them far ahead than other conventional porous materials for tackling the energy related problems based on the high specific surface area, thermal stability, mass productivity, and fast adsorption/desorption kinetics. Possibility of utilizing HPCs derived from a wide range of biomass sources are yet to be employed for next generation technological applications relevant for energy solutions. For example, applications of HPCs in unitized regenerative fuel cells (URFCs), an energy-storage system for uninterrupted power supplies, solar-powered aircraft, and satellites. Bioresourced highly-reproducible 3D morphology with macro-to-mesoporous architecture can resemble intricate structure of its source. Chemical tailoring of such hierarchically-porous, carbon converted, biogenic structure is envisaged to result in high degree of enzyme loading for rapid enzymatic applications. Such carbon structure can also be amplified with carboxylic groups by chemical modification and metal deposition can also open the scope for new applications. Several hydrolase enzymes can be attached to the carboxy-functionalized HPCs via electrostatic attachment and depending on the loading of enzyme, several biocatalytic process can be derived.

HPC coating on other hierarchically structured materials especially magnetic materials with a carbon-coated surface of nanostructured interior can be suitable candidate for Li-ion batteries due to their unique carbon shell. However such materials open significant scope for energy storage applications in other devices as well. Apart from exploring HPCs for application in storing and generation of energy, HPCs are also promising candidates for design catalysts required for selective biomass conversion process. Highly uniform and conformal coatings on surfaces and to infiltrate HPCs derived from biomass will have immense significance. Highly dispersed organic and inorganic species on high surface area material with complex topology is another emerging area, where atomic layer deposition can also be used as alternate method for preparing composites with HPCs.

Enhancement of energy density of supercapacitors depends majorly on optimized porosity or in hybrid devices by employing pseudocapacitive elements. The effects of low charge carrier density of carbon on the total material capacitance is not considered attentively. This can be considered that the increase in density of states (DOS) of low density of charge carriers in carbon

materials leads to a substantial increase in capacitance as the electrode potential increased.¹¹⁴ A significant tool would be to improve the carbon capacitor performance, doping with highly graphitic carbons for stronger degree of electrochemical doping and high skeleton density that may result enhancement of capacitance.

These apart, HPC would find potential applications in the area of enhancement of photocatalytic applications based on the hierarchically organized porous structure which might result slow-photon effect and this photonic structural property of HPCs are yet to be explored for solar thermal storage and artificial photosynthesis. Highly open-up surface structure and hierarchical order would offer framework with properties of accelerating charge collection and separation,¹¹⁵ thus a soft-photocatalytic interface favoring mass transfer may be accessible.

Accessing highly ordered DNA nanowires which are used in waveguides, photodetection, nanophotonic switch, logic device etc. is an attractive field. Controlled evaporation induced self-assembly of DNA aqueous solution on HPC surface may offer aligned DNA nanowires, however the process would depend on the control of flow within the evaporating solution.¹¹⁶ Such controlled evaporation self-assembly would be remarkable and introduce a new avenue for crafting DNA-based HPC nanostructure for applications. Further, hierarchical micro/mesopores in a HPC can act as the drug-loaded nanocontainers to enhance the targeting capability to tumor tissues *in vitro* and inhibited the tumor growth with minimal side effects *in vivo*.¹¹⁷

9. Conclusions

Several energy and environmental solution requires the advance of highly stable, ordered porous nanostructured materials to enhance the performance of the core devices, such as solar and chemical energy storage, separation of gas molecule, pollutant removal from air. Particularly, there is surge in the demand for cutting down the emission level of CO₂ from nonrenewable sources. Short-term goals of carbon capture and sequestration required the absorptive removal of CO₂ from air. Control and optimization of pore geometry, size, volume, surface area and intrinsic basicity at the surface are crucial to achieve efficient CO₂ capture at pre- and post-combustion power stations. High surface area and ultra-high total pore volume are significantly desired for enhanced applications of a hierarchically porous material. Given their rich property, the HPCs are potential candidates for further pore optimization/functionalization for energy storage, especially as super-capacitor electrode materials, methane storage, Li-ion adsorption-desorption

in battery. Obviously selection of precursor plays a critical role in obtaining the desirable porosities in the sp^2 -bonded graphenic carbons¹¹⁸ and N-doping can considerably enhance their CSS application through favorable dipolar interaction with the CO₂ molecules.

In spite of the recent advances on the control of the porosity of carbon materials through mainly hard templating (nano-casting) procedures, and the development of novel carbon materials (graphene, carbon nanotubes), porous carbon with inter-connected pore hierarchy would be the choice for the construction of new generation electrodes for commercial supercapacitors and other energy related applications. To comply with the future energy demands, higher control over the textural properties (pore size, volume, and aspect ratio) is required to maximize so that the power densities can be improved to be suitable for medium to long-term solution. Furthermore, it is essential to reduce the cost of accessing carbon materials by exploring precursor such as biomass, which is low-cost, readily available and renewable, thus will play a key role for various purposes. Strategies for deriving hetero-atom doped carbon from biopolymers and their further application as electrode for use in alkaline super capacitor depends on the controlled ammonia assisted carbonization when starting from a biopolymer without N-content. Strategies of deriving doped-hierarchically porous carbon from biopolymer can also be developed for other elements such P, B etc. Ex situ electrochemical spectroscopy can be used to investigate the evolution of N-functional groups on the surface of the N-doped carbon electrodes in the supercapacitor cell.

The major difficulty which was faced in constructing interconnected pores in macro-meso-microporous carbon system from a non-templating route or from a biorenewable source is controlling the pyrolysis step. Dual templating strategy has been evolved for the construction of hierarchical pore network for crystalline TiO₂ films¹¹⁹ for their applications in photoelectrochemical water-splitting due to structural homogeneity and integrity. Consequently, such strategies to access HPC materials from biopolymers is not yet developed. However, HPCs are not yet been exploited for asymmetric supercapacitor (ASC) with a faradaic electrode as energy source and a capacitive electrode as a power source in which scope for effective approach to increase the cell voltage has plenty of scope. Additionally, potential raw material like bacterial cellulose is yet to be explored for designing HPCs with networking of pores in either as template or precursor for carbon.

References

- 1) J. Aizenberg, J. C. Weaver, M. S. Thanawala, V. C. Sundar, D. E. Morse and P. Fatzl, *Science*, 2005, **309**, 275.
- 2) C. Zou, D. C. Wu, M. Z. Li, Q. C. Zeng, F. Xu, Z. Y. Huang and R. W. Fu, *J. Mater. Chem.*, 2010, **20**, 731.
- 3) B.-Z. Fang, J.-H. Kim, M.-S. Kim, A. Bonakdarpour, A. Lam, D. Wilkinson and J.-S. Yu, *J. Mater. Chem.*, 2012, **22**, 19031.
- 4) H. L. Wang, Y. Yang, Y. Y. Liang, J. T. Robinson, Y. G. Li, A. Jackson, Y. Cui and H. J. Dai, *NanoLett.*, 2011, **11**, 2644.
- 5) Fang, B.-Z.; Kim, M.-W.; Fan, S.-Q.; Kim, J.-H.; Wilkinson, D.; Ko, J.-J.; Yu and J.-S. *J. Mater. Chem.*, 2011, **21**, 8742.
- 6) B.-Z. Fang, J.-H. Kim, M.-S. Kim and J.-S. Yu, *Langmuir*, 2008, **24**, 12068.
- 7) T. L. Kelly, T. Gao and M. J. Sailor, *Adv. Mater.*, 2011, **23**, 1776.
- 8) B.-Z. Fang, J.-H. Kim, M.-S. Kim and J.-S. Yu, *Chem. Mater.*, 2009, **21**, 789.
- 9) P.-Z. Li and Y. Zhao, *Chem. Asian J.*, 2013, **8**, 1680.
- 10) B. Fang, J. H. Kim, M.-S. Kim and J.-S. Yu, *Acc. Chem. Res.*, 2013, **46**, 1397.
- 11) a) S.-W. Woo, K. Dokko, H. Nakano and K. Kanamura, *J. Mater. Chem.*, 2008, **18**, 1674; b) C. Liang, K. Hong, G. A. Guiochon, J. W. Mays and S. Dai, *Angew. Chem. Int. Ed.*, 2004, **43**, 5785; c) Y. Meng, D. Gu, F. Zhang, Y. Shi, H. Yang, Z. Li, C. Yu, B. Tu and D. Zhao, *Angew. Chem. Int. Ed.*, 2005, **44**, 7053.
- 12) a) Z.-Y. Wang, F. Li, N. S. Ergang and A. Stein, *Chem. Mater.*, 2006, **18**, 5543; b) L.-Z. Fan, Y.-S. Hu, J. Maier, P. Adelhelm, B. Smarsly and M. Antonietti, *Adv. Funct. Mater.*, 2007, **17**, 3083; c) M. C. Gutierrez, F. Pic, F. Rubio, J. M. Amarilla, F. J. Palomares, M. L. Ferrer, F. Del Monte and J. M. Rojo, *J. Mater. Chem.*, 2009, **19**, 1236; d) D. Carriazo, F. Pic, M. C. Gutierrez, F. Rubio, J. M. Rojo and F. Del Monte, *J. Mater. Chem.*, 2010, **20**, 773; e) H.-J. Liu, X.-M. Wang, W.-J. Cui, Y.-Q. Dou, D.-Y. Zhao and Y.-Y. Xia, *J. Mater. Chem.*, 2010, **20**, 4223.
- 13) D. W. Wang, F. Li, M. Liu, G. Q. Lu and H. M. Cheng, *Angew. Chem., Int. Ed.*, 2008, **47**, 373.
- 14) A. H. Lu, G. P. Hao, Q. Sun, X. Q. Zhang and W. C. Li, *Macromol. Chem. Phys.*, 2012, **213**, 1107.
- 15) H. Nishihara and T. Kyotani, *Adv. Mater.*, 2012, **24**, 4473.

- 16) Y. Deng, C. Liu, T. Yu, F. Liu, F. Zhang, Y. Wan, L. Zhang, C. Wang, B. Tu, P. A. Webley, H. Wang and D. Zhao, *Chem. Mater.*, 2007, **19**, 3271.
- 17) Z. Wang and A. Stein, *Chem. Mater.*, 2008, **20**, 1029.
- 18) J. Biener, M. Stadermann, M. Suss, M. A. Worsley, M. M. Biener, K. A. Rose and T. F. Baumann, *Energy Environ. Sci.*, 2011, **4**, 656.
- 19) S. L. Candelaria, R. Chen, Y. H. Jeong and G. Cao, *Energy Environ. Sci.*, 2012, **5**, 5619.
- 20) L. Estevez, A. Kelarakis, Q. Gong, E. H. Da'as and E. P. Giannelis, *J. Am. Chem. Soc.*, 2011, **133**, 6122.
- 21) M. C. Guti'erez, M. Jobb'agy, N. Rap'un, M. L. Ferrer and F. Del Monte, *Adv. Mater.*, 2006, **18**, 1137.
- 22) L. Estevez, R. Dua, N. Bhandari, A. Ramanujapuram, P. Wang and E. P. Giannelis, *Energy Environ. Sci.*, 2013, **6**, 1785.
- 23) Y. Xia, Z. Yang and R. Mokaya, *Nanoscale*, 2010, **2**, 639.
- 24) J. Balach, L. Tamnorini, K. Sapag, D. F. Acevedo and C. A. Barbero, *Colloids and Surfaces A*, 2012, **415**, 343.
- 25) C.-H. Huang and R.-A. Doong, *Microporous and Mesoporous Materials*, 2012, **147**, 47-52.
- 26) S. Han and T. Hyeon, *Chem. Commun.*, 1999, 1955.
- 27) N. Pal and A. Bhaumik, *Adv. Coll. Interface Sci.* 2013, **189-190**, 21-41.
- 28) Z. Li, L. Zhang, B. S. Amirkhiz, X. Tan, Z. Xu, H. Wang, B. C. Olsen, C. M. B. Holt and D. Mitlin, *Adv. Energy Mater.*, 2012, **2**, 431.
- 29) B. G. Choi, M. Yang, W. H. Hong, J. W. Choi and Y. S. Huh, *ACS Nano*, 2012, **6**, 4020.
- 30) H. Jiang, P. S. Lee and C. Li, *Energy Environ. Sci.*, 2013, **6**, 41.
- 31) L. Qie, W. Chen, H. Xu, X. Xiong, Y. Jiang, F. Zou, X. Hu, Y. Xin, Z. Zhang and Y. Huang, *Energy Environ. Sci.*, 2013, **6**, 2497.
- 32) B. Li, W. Han, B. Jiang and Z. Lin, *ACS Nano*, 2014, **8**, 2936.
- 33) M. Sevilla and A. B. Fuertes, *Energy Environ. Sci.*, 2011, **4**, 1765.
- 34) W. Shen, Y. He, S. Zhang, J. Li and W. Fan, *ChemSusChem*, 2012, **5**, 1274.
- 35) D. Wu, C. M. Hui, H. Dong, J. Pietrasik, H. J. Ryu, Z. Li, M. Zhong, H. He, E. K. Kim and M. Jaroniec, *Macromolecules*, 2011, **44**, 5846.
- 36) Q. Zeng, D. Wu, C. Zou, F. Xu, R. Fu, Z. Li, Y. Liang and D. Su, *Chem. Commun.*, 2010, **46**, 5927.

- 37) X. Huang, S. Kim, M. S. Heo, J. E. Kim, H. Suh and I. Kim, *Langmuir*, 2013, **29**, 12266.
- 38) Z. Q. Li, C. J. Lu, Z. P. Xia, Y. Zhou and Z. Luo, *Carbon*, 2007, **45**, 1686.
- 39) a) S. Dutta, *RSC Adv.*, 2012, **2**, 12575; b) S. Dutta, S. De and B. Saha, *ChemPlusChem*, 2012, **4**, 259.
- 40) a) Y. Huang, H. Cai, D. Feng, D. Gu, Y. Deng, B. Tu, H. Wang, P. A. Webley and D. Zhao, *Chem. Commun.*, 2008, 2641; b) M. C. Gutierrez, F. Pico, F. Rubio, M. Amarilla, F. J. Palomares, M. L. Ferrer, F. Del Monte and J. M. Rojo, *J. Mater. Chem.*, 2009, **19**, 1263.
- 41) P. Zhang, J. Yuan, T.-P. Fellingner, M. Antonietti, H. Li and Y. Wang, *Angew. Chem. Int. Ed.*, 2013, **52**, 6028.
- 42) D. Qian, C. Lei, G.-P. Hao, W.-C. Li and A.-H. Lu, *ACS Appl. Mater. Interfaces*, 2012, **4**, 6125.
- 43) J. Wang and S. Kaskel, *J. Mater. Chem.*, 2012, **22**, 23710.
- 44) X. He, R. Li, J. Qiu, K. Xie, P. Ling, M. Yu, X. Zhang and M. Zheng, *Carbon*, 2012, **50**, 4911.
- 45) B. Xu, S. Hou, G. Cao, F. Wu and Y. Yang, *J. Mater. Chem.*, 2012, **22**, 19088.
- 46) B. Xu, S. Hou, G. Cao, M. Chu and Y. Yang, *RSC Adv.*, 2013, **3**, 17500.
- 47) H. Zhong, F. Xu, Z. Li, R. Fu and D. Wu, *Nanoscale*, 2013, **5**, 4678.
- 48) L. Wei, M. Sevilla, A. B. Fuertes, R. Mokaya and G. Yushin, *Adv. Funct. Mater.*, 2012, **22**, 827.
- 49) N. Lin, J. Huang and A. Dufrense, *Nanoscale*, 2012, **4**, 3274.
- 50) S. J. Eichhorn, *Soft Mat.*, 2011, **7**, 303.
- 51) K. E. Shopsowitz, H. Qi, W. Y. Hamad and M. J. MacLachlan, *Nature*, 2010, **468**, 422.
- 52) a) E. Raymundo-Pinero, F. Lerous and F. Beguin, *Adv. Mater.*, 2006, **18**, 1877.; b) S. H. Guo, J. H. Peng, W. Li, K. B. Yang, L. B. Zhang, S. M. Zhang and H. Y. Xia, *Appl. Surf. Sci.*, 2009, **255**, 8443.
- 53) F. Zhang, K. X. Wang, G. D. Li and J. S. Chen, *Electrochem. Commun.*, 2009, **11**, 130.
- 54) W. Z. Shen, Z. F. Qin, H. G. Wang, Y. H. Liu, Q. J. Guo and Y. L. Zhang, *Colloids Surf. A*, 2008, **316**, 313.
- 55) S. Dutta, A. K. Patra, S. De, A. Bhaumik and B. Saha, *ACS Appl. Mater. Interfaces*, 2012, **4**, 1560.
- 56) M. Buaki-Sogo, M. Serra, A. Primo, M. Alvaro and H. Garcia, *ChemCatChem*, 2013, **5**, 513.

- 57) M. Chtchigrovsky, Y. Lin, K. Ouchaou, M. Chaumontet, M. Robitzer, F. Quignard and F. Taran, *Chem. Mater.*, 2012, **24**, 1505.
- 58) A. Primo, M. Liebel and F. Quignard, *Chem. Mater.*, 2009, **21**, 621.
- 59) X.L. Wu, L.-L. Chen, S. Xin, Y.-X. Yin, Y.-G. Guo, Q.-S. Kong and Y.-Z. Xia, *ChemSusChem*, 2010, **3**, 703.
- 60) M. Latorre-Sanchez, A. Primo and H. Garcia, *Angew. Chem. Int. Ed.*, 2013, **52**, 1.
- 61) Y. Liang, D. Wu and R. Fu, *Sci. Rep.*, 2013, **3**, 1119.
- 62) Zhu, H.; Wang, X. L.; Yang, F.; Yang and X. R. *Adv. Mater.*, 2011, **23**, 2745.
- 63) Wu, F. C.; Tseng, R. L.; Hu, C. C.; Wang and C. C. *J. Power Sources.*, 2004, **138**, 351.
- 64) Chen, W. X.; Zhang, H.; Huang, Y. Q.; Wang and W. K. *J. Mater. Chem.*, 2010, **20**, 4773.
- 65) L. Wei, M. Sevilla, A. B. Fuertes, R. Mokaya and G. Yushin, *Adv. Energy Mater.*, 2011, **1**, 356.
- 66) R. Wang, P. Wang, X. Yan, J. Land, C. Peng and Q. Xue, *ACS Appl. Mat. Interfaces*, 2012, **4**, 5800.
- 67) S.-H. Du, L.-Q. Wang, X.-T. Fu, M.-M. Chen and C.-Y. Wang, *Bioresource Technol.*, 2013, **139**, 406.
- 68) J. Huang and T. J. Kunitake, *J. Am. Chem. Soc.*, 2003, **125**, 11834.
- 69) J. Pan, W. Y. Hamad and S. K. Strauss, *Macromolecules*, 2010, **43**, 3851.
- 70) J. F. Revol, L. Godbout and D. G. Gray, *J. Pulp Pap. Sci.*, 1998, **24**, 146.
- 71) K. E. Shopsowitz, W. Y. Hamad and M. J. MacLachlan, *Angew. Chem. Int. Ed.*, 2013, **50**, 10991.
- 72) A. Y. Liu and M. L. Cohen, *Science*, 1989, **245**, 841 ; b) Y. D. Xia and R. Mokaya, *Adv. Mater.*, 2004, **16**, 1553.
- 73) D. Hulicova-Jurcakova, M. Seredych, G. Q. Lu and T. J. Bandosz, *Adv. Funct. Mater.*, 2009, **19**, 438.
- 74) L. F. Chen, X. D. Zhang, H. W. Liang, M. Kong, Q. F. Guan, P. Chen, Z. Y. Wu and S. H. Yu, *ACS Nano*, 2012, **6**, 7092.
- 75) M. Zhong, E. K. Kim, J. P. McGann, S.-E. Chun, J. F. Whitacre, M. Jaroniec, K. Matyjaszewski and T. Kowalewski, *J. Am. Chem. Soc.*, 2012, **134**, 14846.
- 76) Z. Li, Z. Xu, X. Tan, H. Wang, C. M. B. Holt, T. Stephenson, B. C. Olsen and D. Mitlin, *Energy Environ. Sci.*, 2013, **6**, 871.

- 77) Z. Wen, X. Wang, S. Mao, Z. Bo, H. Kim, S. Cui, G. Lu, X. Feng and J. Chen, *Adv. Mater.*, 2012, **24**, 5610.
- 78) H. R. Byon, B. M. Gallant, S. W. Lee and Y. Shao-Horn, *Adv. Funct. Mater.*, 2013, **23**, 1037.
- 79) Y. Mao, H. Duan, B. Xu, L. Zhang, Y. Hu, C. Zhao, Z. Wang, L. Chen and Y. Yang, *Energy Environ. Sci.*, 2012, **5**, 7950.
- 80) D. Hulicova-Jurcakova, A. M. Puziy, O. I. Poddubnaya, F. Surez-Garcia, J. M. D. Tascn and G. Q. Lu, *J. Am. Chem. Soc.*, 2009, **131**, 5026.
- 81) J. Zhang, X. Liu, R. Blume, A. H. Zhang, R. Schlogl and D. S. Su, *Science*, 2008, **322**, 73.
- 82) D. W. Wang, F. Li, Z. G. Chen, G. Q. Lu and H. M. Cheng, *Chem. Mater.*, 2008, **20**, 7195.
- 83) D. Hulicova, J. Yamashita, Y. Soneda, H. Hatori and M. Kodama, *Chem. Mater.*, 2005, **17**, 1241.
- 84) C. O. Ania, V. Khomenko, E. Raymundo-Pinero, J. B. Parra and F. Beguin, *Adv. Funct. Mater.*, 2007, **17**, 1828.
- 85) Y. J. Kim, Y. Abe, T. Yanaglura, K. C. Park, M. Shimizu, T. Iwazaki, S. Nakagawa, M. Endo and M. S. Dresselhaus, *Carbon*, 2007, **45**, 2116
- 86) K. Jurewicz, K. Babel, R. Pietrzak, S. Delpeux and H. Wachowska, *Carbon*, 2006, **44**, 2368
- 87) D.-W. Wang, F. Li, L.-C. Yin, X. Lu, Z.-G. Chen, I. R. Gentle, G.-Q. Lu and H.-M. Cheng, *Chem. Eur. J.*, 2012, **18**, 5345.
- 88) a) L. Meng and X. Junmin, *J. Phy. Chem. C*, 2014, **118**, 2507; b) C. Ma, J. Shi, Y. Song, D. Zhang, X. Zhai, M. Zhong, Q. Guo and L. Liu, *Int. J. Hydrogen Energ.* 2012, **7**, 7587.
- 89) G.-P. Hao, W.-C. Li, D. Qian, G.-H. Wang, W.-P. Zhang, T. Zhang, A.-Q. Wang, F. Schuth, H.-J. Bongard and A.-H. Lu, *J. Am. Chem. Soc.*, 2011, **133**, 11378.
- 90) a) G.-P. Hao, W.-C. Li, D. Qian and A.-H. Lu, *Adv. Mater.*, 2010, **22**, 853.
- 91) M. Nandi, K. Okada, A. Dutta, A. Bhaumik, J. Maruyama, D. Derks and H. Uyama, *Chem. Commun.*, 2012, **48**, 10283.
- 92) D. Carriazo, M. C. Gutierrez, F. Pico, J. M. Rojo, J. L. G. Fierro, M. L. Ferrer and F. Del Monte, *ChemSusChem*, 2012, **5**, 1405.
- 93) D. Carriazo, M. C. Gutierrez, M. L. Ferrer and F. Del Monte, *Chem. Mat.*, 2010, **22**, 6146.
- 94) D.-C. Guo, J. Mi, G.-P. Hao, W. Dong, G. Xiong, W.-C. Li and A.-H. Lu, *Energy Environ. Sci.*, 2013, **6**, 652.

- 95) T. Wang, K. S. Lackner and A. Wright, *Environ. Sci. Technol.*, 2011, **45**, 6670.
- 96) H. He, W. Li, M. Zhong, D. Konkolewicz, D. Wu, K. Yaccato, T. Rappold, G. Sugar, N. E. David and K. Matyjaszewski, *Energy Environ. Sci.*, 2013, **6**, 488.
- 97) A. Modak, M. Nandi, J. Mondal and A. Bhaumik, *Chem. Commun.*, 2012, **48**, 248.
- 98) A. Dutta, M. Nandi, M. Sasidharan and A. Bhaumik, *ChemPhysChem*, 2012, **13**, 3218-3222.
- 99) X. L. Ji, K. T. Lee and L. F. Nazar, *Nature Mater.*, 2009, **8**, 500.
- 100) B. Ding, C. Yuan, L. Shen, G. Xu, P. Ni and X. Zhang, *Chem. Eur. J.* 2013, **19**, 1013.
- 101) Z. Chen, J. Wen, C. Yan, L. Rice, H. Sohn, M. Shen, M. Cai, B. Dunn and Y. Lu, *Adv. Energy Mater.*, 2011, **1**, 551.
- 102) J. Chmiola, G. Yushin, Y. Gogotsi, C. Portet, P. Simon and P. L. Taberna, *Science*, 2006, **313**, 1760.
- 103) W. Xing, C. Huang, S. Zhuo, X. Yuan, G. Wang, D. Hulicova-Jurcakova, Z. Yan and G. Lu, *Carbon*, 2009, **47**, 1715.
- 104) W. Xing, C. C. Huang, S. P. Zhuo and X. Yuan, *Langmuir*, 2009, **25**, 7783.
- 105) H. Yamada, I. Moriguchi and T. Kudo, *J. Power Sources*, 2008, **175**, 651.
- 106) C. Largeot, C. Portet, J. Chmiola, P. L. Taberna, Y. Gogotsi and P. Simon, *J. Am. Chem. Soc.*, 2008, **130**, 2730.
- 107) L. Eliad, G. Salitra, A. Soffer and D. Aurbach, *J. Phys. Chem. B*, 2001, **105**, 6880.
- 108) G. Wang, E. Johannessen, C. R. Kleijn, S. W. de Leeuw, M. -O. Coppens, *Chem. Eng. Sci.*, 2007, **62**, 5110.
- 109) G. Wang, M.-O. Coppens, *Chem. Eng. Sci.*, 2010, **65**, 2344.
- 110) Y. H. Deng, C. Liu, T. Yu, F. Liu, F. Q. Zhang, Y. Wan, L. Zhang, C. Wang, B. Tu, P. A. Webley, H. Wang, D. Zhao, *Chem. Mater.*, 2007, **19**, 3271.
- 111) a) J. S. Lee, X. Q. Wang, H. M. Luo, G. A. Baker and S. Dai, *J. Am. Chem. Soc.*, 2009, **131**, 4596; b) X. Q. Wang and S. Dai, *Angew. Chem. Int. Ed.*, 2010, **49**, 6664; c) W. Yang, T. P. Feller and M. Antonietti, *J. Am. Chem. Soc.*, 2011, **133**, 206; d) J. S. Lee, X. Q. Wang, H. M. Luo and S. Dai, *Adv. Mater.*, 2010, **22**, 1004.
- 112) J. Wei, D. Zhou, Z. Sun, Y. Deng, Y. Xia and D. Zhao, *Adv. Funct. Mat.*, 2013, **23**, 2322.
- 113) J. Schuster, G. He, B. Mandlmeier, T. Yim, K. T. Lee, T. Bein and L. F. Nazar, *Angew. Chem. Int. Ed.*, 2012, **51**, 3591.
- 114) P. Ganesh, P. R. C. Kent and V. Mochalin, *J. Appl. Phys.*, 2011, **110**, 073506.

- 115) J. Zhang, J. Sun, K. Maeda, K. Domen, P. Liu, M. Antonietti, X. Fu and X. Wang, *Energy Environ. Sci.*, 2010, **4**, 675.
- 116) B. Li, W. Han, M. Byun, L. Ahu, Q. Zou and Z. Lin, *ACS Nano*, 2013, **7**, 4326.
- 117) Z. Luo, X. W. Ding, Y. Hu, S. J. Wu, Y. Xiang, Y. F. Zeng, B. L. Zhang, H. Yan, H. C. Zhang, L. L. Zhu, J. J. Liu, J. H. Li, K. Y. Cai and Y. L. Zhao, *ACS Nano*, 2013, **7**, 10271-10284.
- 118) G. Srinivas, V. Krungleviciute, Z.-X. Guo and T. Yildirim, *Energy Environ. Sci.*, 2014, **7**, 335.
- 119) R. Zhang, D. Shen, M. Xu, D. Feng, W. Li, G. Zheng, R. Che, A. A. Elzatahry and D. Zhao, *Adv. Eng. Mater.*, 2014, DOI: 10.1002/aenm.201301725.

Broader Context

Inter-connected pore network in hierarchically porous carbons (HPCs) consisting of macro, meso, and micropores are currently attractive candidate for advanced technological applications ranging from electrochemical supercapacitor, Li batteries, solar cell, and fuel cells. However, despite the ceaseless development on porous carbons, limited success has been achieved in synthesis of HPCs by conventional hard-templating method. Besides, non-renewable carbon sources were utilized for the fabrication of HPCs. In a long-term perspective, looking for biorenewable carbon sources for HPCs is essential along with developing unconventional non-templating route that retains framework of pore-networks and also offer high specific surface areas, desired pore size and shape. We herein review, how polymer, block-copolymers, and biopolymers have been utilized as carbon source to offer HPCs of versatile nanostructures. Hetero-atom doped mesoporous carbon monolith with hierarchical pores can be accessible from N-containing polymeric resins. The derived HPCs demonstrated synergistic effect of macro-, meso- and microporosity in energy related applications where ion-transport, buffering, electrical double layer enhancement, and ion diffusion play significant roles. The effect of interconnected pores in CO₂ adsorption and photonic crystal sensor were described. Advantages of HPC over OMC was discussed. Current progress of HPCs derived from biopolymers, challenges, and future applications were critically presented.